Ecological Modelling 339 (2016) 96–125

Contents lists available at ScienceDirect

Ecological Modelling

journal homepage: www.elsevier.com/locate/ecolmodel

Emergy baseline for the Earth: A historical review of the science and a new calculation

Daniel E. Campbell*

USEPA, Office of Research and Development, National Health and Environmental Effects Research Laboratory, Atlantic Ecology Division, 27 Tarzwell Drive, Narragansett, RI 02882, USA

ARTICLE INFO

Article history:
Received 28 April 2015
Received in revised form
14 December 2015
Accepted 16 December 2015
Available online 20 January 2016

Keywords:
Planetary emergy baseline
Emergy evaluation
Solar exergy
Tidal geopotential energy
Deep Earth heat flow

ABSTRACT

Quantifying the emergy baseline of the Earth is a practical necessity for emergy evaluations, because it serves as a unified basis for determining transformities of the available energy storages and flows of the geobiosphere. The current debate over the value and significance of the planetary baseline has been in progress since 1998, when the author first brought new data on geopotential energy formation in the world oceans to H.T. Odum's attention. In this paper, past studies of the baseline were reviewed and errors in data translation and model formulation were found to be sufficient to justify a new calculation. A fundamental epistemological obstacle to establishing a unified planetary baseline (i.e., the production functions for deep Earth heat and tide as a function of solar radiation are unknown) is overcome by using the transitive property of equalities to estimate equivalences between solar radiation and Earth's deep heat exergy flows (4200 solar equivalent joules per joule, seJ J^{-1}) and between the exergy of solar radiation and the tidal exergy dissipated in the oceans (35,400 seJ J^{-1}). At present, the planetary baseline for the Earth with its ice-covered, polar oceans is approximately 1.16×10^{25} seJ y^{-1} and the distribution of the emergy or the organizing power of the inputs is: 1/3 solar radiation, 1/3 deep Earth heat and 1/3 tidal geopotential energy. In addition, the planetary baseline has been remarkably stable over the past 555,000,000 y ($1.00 \times 10^{25} \pm 1.13 \times 10^{24}$ seJ y^{-1} or within ±11%). The tidal exergy dissipated in the world oceans over this time varies from 31% to 155% of its present value largely due to the changing efficiency of the Earth as a "machine" for generating tidal exergy. Close correspondence of the value and properties of this new baseline with the principles of Energy Systems Theory indicates that it should be preferred over prior determinations.

1. Introduction

One of the greatest problems confronting people who make public policy decisions is how to fairly weigh the value of disparate quantities in decision-making, so that maximum benefits or minimum losses can be achieved upon making a choice among alternatives. One common approach to solve this problem is through economics, i.e., a market or nonmarket monetary value is determined based on the willingness of people to pay or accept payment for a product or service (Breidert et al., 2006). This method works fairly well when a value must be assigned to items of common use among people; however, economic methods are not as useful or as accurate when value must be assigned to the work of the environment or in cases where overall public well-being is of concern (Campbell, 2014).

H.T. Odum's fundamental insights into the structure and function of all systems lay in the realization that the transformations of energy potentials underlie all actions and that they are hierarchically organized. As a result of this fact, an accounting procedure establishing value, in terms of the available energy required to produce an item, i.e., its "production cost", can be carried out for anything, if the production function is known. Building on this insight, Odum (1996) proposed an evaluation system that is capable of representing the value of environmental, economic, and social "goods and services" with a common, comprehensive measure, emergy. Emergy is an accounting quantity that tracks all of the available energy (i.e., exergy)[1] of one kind used in the past, both directly and indirectly, to make a product or service (Odum, 1996). Its unit is the emjoule abbreviated sej (Odum, 1996) or semj

* Corresponding author. Tel.: +1 0114017823195; fax: +1 0114017823030.
E-mail address: campbell.dan@epa.gov

[1] In this paper, available energy and exergy are used interchangeably to refer to the same quantity, i.e., the work that can be performed by an energy potential, when it is reduced to its ground state.

http://dx.doi.org/10.1016/j.ecolmodel.2015.12.010

(Scienceman, 1987). It is a solar equivalent joule of available energy that has been used in the past to create a product or service. Since the sun is by far the largest source of energy and of available energy entering the Earth, it is logical that the solar joule was chosen as the base energy type (Odum, 1996).

Solar emjoules can be used to quantify all products of the transformations of available energy delivered to the geobiosphere through the planetary baseline. To perform this accounting using emergy, the production process for an item must be known and the many disparate forms of available energy that are required in the process must be converted to available energy of a single kind, i.e., of a single quality, such as, solar equivalent joules. However, the Earth's deep heat and tidal exergies cannot be quantified as products of the exergy of solar radiation (Raugei, 2013). For this reason, in this study, we follow Brown and Ulgiati (2016) in recognizing Raugei's assertion that the emergy baseline of the Earth must be quantified as solar equivalent joules, seJ, rather than as solar emjoules, sej, the measure of solar emergy.

Since all natural phenomena are organized as a hierarchical interconnected system of energy flows and interactions, for practical reasons, spatial and temporal boundaries must be set for every analysis. A "window of observation" is a device that can be used to establish the spatial and temporal limits of a system. For example, temporal limits can be established in the frequency domain by the maximum time of observation and the minimum time between observations (Campbell, 1984). In order to make decisions for society, the geobiosphere (Odum, 1996, Fig. 3.1; Brown and Ulgiati, 2010) must be evaluated, because it is the system of which society is a part. Furthermore, the larger scale of evaluation needed to understand the geobiosphere is that of the whole Earth. Thus, the largest spatial dimension for our decision-making will be no larger than the scale of the geobiosphere, or the Earth's surface with atmospheric and solid Earth boundaries functionally defined, and the temporal boundary will be no longer than the period of time over which the geobiosphere can exist. Although this time is uncertain, it is roughly from 3.6 to 3.5×10^9 years before the present, BP (i.e., from the time of the stromatolites, which provide the first fossil evidence of life in the geologic record) to some unknown time in the future. One estimate of the time at which the planet will no longer support life is provided by Sorokhtin et al. (2011), who predict that 0.6×10^9 years into the future, the release of free oxygen from the interior of the Earth may result in oxygen concentrations at the surface that are too great for life to exist. In both cases the upper limit of the spatial and temporal windows of observation will be determined by the sampling interval (Campbell, 1984), because this defines the size and frequency of observable phenomena.

In emergy evaluations, the track-sum method (Tennenbaum, 1988) or some variation of it (Li et al., 2010; Le Corre and Truffet, 2012) is used to trace the flow of available energy through a web of production functions to quantify the available energy required for a product or service by summing the inputs without double counting. To accomplish this one type of available energy must be chosen as a base and most emergy evaluations of environmental systems choose solar joules. Many products and services observed on the Earth can be traced in large part to the transformations of available solar energy, e.g., solar and wind energy → the transpiration[2] of plants → gross primary production (GPP) → deer biomass → Native American hunters → egalitarian social structures (Ojibwa, 2012); however, the Earth system would not exist in its present form if the sun was the only energy source operating the planet. In fact, the available energy flow from deep heat generated within the Earth and the available energy flow supplied by the gravitational attraction of the Moon and Sun are essential for the operation of Earth processes, e.g., tectonic processes and tidal transport and mixing, in the former and latter case, respectively. These three disparate sources of available energy to the Earth are quasi-independent[3] and as a result they are not amenable to the standard track-sum method for determining the emergy of their quantities in terms of the solar joules required. Nevertheless, establishing an emergy baseline for the Earth that unifies these three sources under a common unit is a practical necessity to carryout emergy accounting in a uniform manner for all systems within the geobiosphere.

If emergy accounting is to fulfill the requirements given above, equivalence must be established between the three major[4], irreducible, quasi-independent available energy inputs to the Earth, i.e., solar radiation, S, deep Earth heat, E, and the gravitational attraction of the Moon and Sun or the tides, G. If the base unit for emergy evaluations is the solar joule, the problem reduces to establishing equivalence between solar radiation and the available energy of Earth's deep heat flow and between solar radiation and the available energy dissipated by the tides in the oceans, i.e., calculating the solar transformities of deep Earth heat and oceanic tidal dissipation. Once these equivalences are established, an emergy baseline for the Earth can be determined by multiplying the solar transformities of solar radiation, deep Earth heat, and tidal dissipation by their respective flows of available energy that drive the geobiosphere. The emergy baseline of the Earth or the solar equivalent joules per year, seJ y^{-1}, inflowing to the Earth's geobiosphere, once established, can be used to determine the transformities (sej J^{-1}) of all planetary processes, e.g., the annual available energy flows of the wind, rain, waves, etc. The primary and secondary emergy inputs are the basis for calculating all transformities and other emergy per unit values, e.g., specific emergies, sej g^{-1}, emergy to money ratios, sej $\$^{-1}$ etc. of storages and flows within the Earth's geobiosphere.

The goal of this paper is to provide the community of scientists with an accurate estimate of the planetary emergy baseline of the Earth. In the process, it will be demonstrated that the planetary emergy baseline of the Earth is not entirely arbitrary and that the choice of a baseline is a matter that ultimately reflects on the scientific integrity of emergy research, if not the practical outcomes of emergy evaluations. The objectives of this paper are first to examine the data and models upon which past emergy baseline calculations have been made as a way to demonstrate the need for a new calculation of the planetary baseline, and second, to carry out that calculation, by estimating the value of the baseline in the present and from 555,000,000 years BP[5] to the present time using Euclid's Axiom: two things, which are equal to the same thing, also equal

[2] In emergy evaluations, transpiration is assumed to completely capture the emergy basis for plant production, because it integrates, solar radiation, wind energy, vapor pressure gradients in air and fresh water (Odum, 1996).

[3] In theory, solar radiation and the mass of the Earth might be traced from a common energy source (gravity) through the origin and evolution of the solar system, but the production functions are unknown or uncertain. This method of tracking the emergy inputs was explored with Steve Tennenbaum, but it was not used in this study.

[4] Over the long run the high energy radiation and particles carried by the "solar windäre generated by the same processes on the sun that are responsible for incoming solar radiation, thus to add additional emergy for this input would be double counting (Odum, 1996). Other minor sources of energy and mass entering the Earth are not considered in this analysis, e.g., mass influx of interstellar matter.

[5] Five hundred and fifty-five million years BP was chosen because it is the midpoint of the period from 570 to 540×10^6 y BP, which Kagan (1997) characterized as the Early Cambrian Age; a time when multicellular animal life first began to dominate the Earth, e.g., a fully developed fauna of trilobites and brachiopods was present in the fossil record by 542×10^6 y BP. At this time, the continents already had undergone several cycles of convergence and divergence and Earth heat flows were in a slow, stable decline (Sorokhtin et al., 2011). Plants had not yet evolved and the continents were barren. However, the seas were full of life, and increasing oxygen concentrations in the sea may have given rise to the Cambrian "Explosionöf multicellular animal life. http://www.ucmp.berkeley.edu/cambrian/cambrian.php.

one another (Heath, 1908, see http://www.sfu.ca/ swartz/euclid.htm).

2. A historical review of the science related to the calculation of planetary emergy baselines

This section includes a historical review of the science related to the calculation of the Earth's planetary emergy baseline with a focus on the evolution of the idea and on errors in past calculations. The historical context for the baseline is not well-known and has not been published in detail in existing peer-reviewed publications; therefore, it is presented here. The numerical and conceptual errors found in past calculations of the baseline and the mixing of time scales in the two equation-two unknown models used in Odum (2000) to solve for the transformities of deep Earth heat and tidal geopotential energy have not been identified in earlier studies.

2.1. The Earth's emergy baseline: Evolution of an idea

A chronological account of the evolution of the idea of environmental accounting and the concomitant need to specify a baseline for making emergy calculations is given in Appendix E of Odum (1996). In the early stages of thought on this subject, Odum realized that higher quality components and flows within an ecosystem could be expressed in terms of fundamental units of lower quality that were required for their production. Initially, this idea was manifested as an accounting method based on organic matter with 1000 kilocalories of sunlight required for a kilocalorie of organic matter. A second major advance in the development of emergy methods occurred during Odum's trips to New Zealand (1980–1982). At this time, he recognized that there was a hierarchy of energy transformations on the surface of the Earth, such that the solar driven processes of the oceanic and atmospheric heat engines carry rain, wind and waves onto the continents and in this way the solar energy of global processes would be "embodied" in land productivity (Odum, 1996). Thus, the rain falling on land must be of higher transformity[6] than that falling on the oceans, because of the available energy required for its hierarchical convergence onto the land. In 1983, while visiting the International Institute for Applied Systems Analysis (IIASA) in Austria, Odum made a third breakthrough in his understanding of environmental accounting for the Earth (Odum and Odum, 1983). When he returned to Gainesville, FL, after that trip, he was beaming because he had come to understand how equivalence between solar energy and the geologic heat sources from within the Earth could be made. These calculations resulted in a baseline for the Earth of 8.0×10^{24} seJ y^{-1}.

The present form of the planetary baseline, in which the annual emergy inflow from solar radiation, deep Earth heat and the tides are all quantified, was established more than a decade after the Odum's visited IIASA with the publication of Odum (1996). In this book, he added an estimate of the emergy of tidal currents to earlier estimates of the emergy supplied to the Earth through solar radiation and the Earth's deep heat flow, which resulted in an 18% increase in the planetary baseline, from 8.0×10^{24} to 9.44×10^{24} seJ y^{-1}. At this time, Odum recognized that studies by specialists in geophysics might be required to refine his initial baseline calculations. However, he argued that the absolute value of the planetary baseline might not be so important, since the results of emergy analyses are relative to a given baseline and, in general, will not change with a change in the reference level (Odum, 1996). In 1996, he thought that "it may be desirable not to change the baseline further, since it does not affect the differences on which EMERGY accounting is based." Nonetheless, it seems obvious that a change would be warranted, if scientists develop an improved understanding of the geophysics of the Earth or if substantive errors are identified in the original calculations.

2.1.1. Changes in the planetary baseline after 1996

An inconsistency in Odum's calculation of the 9.44 baseline arose, because the emergy of the tides had been estimated in a different manner from that of the Earth's deep heat. Specifically, Odum's elegant determination of the equivalence between solar radiation and deep Earth heat relied on Euclid's principle, which is equivalent to the transitive law of equalities in logic (i.e., If $a = b$ and $b = c$; then $a = c$; http://www.britannica.com/EBchecked/topic/602836/transitive-law). However, at that time, Odum did not have a parallel process to evaluate the equivalence between the tidal energy and solar radiation, so this relationship was estimated by assuming that the solar transformity of tidal currents was equal to that of the physical energy of streams (Table 3.2 in Odum, 1996). This inconsistency was resolved when Campbell (1998) found data on the generation of geopotential energy in the world oceans (Oort et al., 1989) that allowed the transformity of the tides to be estimated in a manner similar to that used for the deep heat of the Earth (Campbell and Odum, Appendix B in Campbell, 1998). Despite errors in their interpretation of the geopotential energy calculations of Oort et al. (1989), the work of Campbell and Odum (1998) led to a new direction in the calculation of the planetary baseline that was focused on the application of uniform calculation methods. A key question raised by Odum in this study was whether the Earth's deep heat flow contributed to the tidal component of the geopotential energy of the world oceans. As a result of his arguments, Campbell (1998) calculated a planetary baseline of 10.57×10^{24} seJ y^{-1} for use in an emergy evaluation of the State of Maine, by assuming that the geopotential energy of the world oceans was created by the interaction of S, G, and E and the Earth Cycle is driven by the interaction of S and E.

Odum and Campbell took divergent approaches to calculating the baseline from their initial study. Odum (2000) and Odum et al. (2000) calculated the equivalence between solar energy and the Earth's deep heat flow and between solar energy and the available energy of the tides by setting up a system of two equations to solve for the two unknowns. The structure of these equations implied that the energy inputs to the Earth's geobiosphere supplied by solar radiation, the gravitational attraction of the Moon and Sun and the deep heat from the Earth are completely coupled through multiplicative interactions to (1) produce "crustal" heat flow and (2) produce the geopotential of the world oceans. In a completely coupled system, these two equations, when evaluated, give a baseline of 15.83×10^{24} seJ y^{-1}. In these two publications, Odum converted many existing transformities to the 15.83 baseline and calculated many new ones relative to this baseline.

In the meantime, Campbell (2000a) made two estimates of the planetary baseline using the numbers from Odum (1996) under the assumption that the geopotential energy of the world oceans is the same regardless of how it is generated; and therefore, it can be split into two products with equal transformity (a variation of Euclid's principle mentioned above). Without changing Odum's determination of the transformity of Earth's deep heat, Campbell (2000a) set up two equations: one for the transformity of the tide, if only solar radiation (S) and the gravitational attraction of the Moon and Sun (G) were responsible for generating the geopotential of the world oceans, and a second for the case in which the emergy of the sun, the emergy of the Earth's deep heat (E) and the emergy of the tides determine the geopotential of the world oceans. When these relationships were evaluated the former case

[6] Higher transformity or higher emergy per unit exergy flows (sej J^{-1}) are of higher quality because they can do more different kinds of work, e.g., rain on land can support higher plant productivity, chemical weathering, etc.

Table 1
Fraction of empower inflow attributable to each independent emergy source for different configurations of the inputs to the baseline. Source configurations are shown as a combination of the letters S, G, and E (S, solar energy, G, gravitational attraction of the Moon and Sun and, E, Earth deep heat) with the configuration used to estimate the transformity of crustal heat given by the first set of letters and the configuration for the geopotential of the world oceans by the second set. All combinations are shown, whether used in a paper or not.

Source	SGE, SGE[1]	SGE, SGE[2]	SE, SGE[3]	SGE, SG	SE, SG[4]
Earth	0.509	0.217	0.385	0.509	0.44
Sun	0.248	0.237	0.372	0.372	0.42
Tide	0.243	0.546	0.243	0.119	0.136
Baseline (seJ y^{-1})	15.83×10^{24}	15.2×10^{24}	10.57×10^{24}	10.57×10^{24}	9.26×10^{24}
Relative Organizing Power					
Sun/Tide	1.021	0.434	1.531	3.126	3.088
Sun/Earth	0.487	1.092	0.966	0.731	0.955

(1) Odum (2000). (2) Brown and Ulgiati (2010). (3) Campbell & Odum in Campbell (1998). (4) Campbell (2000a) after Odum (1996).

gave a planetary baseline of 9.26×10^{24} seJ y^{-1} and the latter a baseline of 10.57×10^{24} seJ y^{-1}. Furthermore, Campbell argued that the former baseline was suitable for most emergy evaluations on short time scales (<10,000 y) and the later would only be relevant over long time periods (≫10, 000 y), when the slow movement of the configuration of the Earth's continents might be great enough to noticeably change the amount of tidal energy generated on Earth.

Campbell et al. (2005) revisited the planetary baseline, because three different emergy baselines were being commonly employed by emergy researchers: (1) Odum's 9.44 baseline (Odum, 1996), (2) Odum's 15.83 baseline (Odum, 2000) or (3) Campbell's 9.26 baseline (Campbell, 2000a), which is the 9.44 baseline corrected by using a consistent method to establish both the transformity of the tides and that of the Earth's deep heat. Campbell et al. (2005) pointed out that in using the method of setting up two equations to solve for two unknowns, the various emergy baselines for the Earth result from using different configurations and combinations of the three main independent emergy sources operating the Earth's geobiosphere to establish the equivalences between solar radiation and the energy inflows of Earth deep heat and tides. These authors concluded that based on the state of knowledge at that time, more than one baseline might be plausible and that emergy researchers should report the baseline used in all studies, and insure that all transformities in a study are expressed relative to that baseline.

Next, Campbell et al. (2010) examined the question, "Is the emergy baseline for the Earth arbitrary?" They reviewed the arguments as to why the baseline might be considered to be arbitrary: (1) the results of an emergy analysis are expressed relative to a baseline and, all other things being equal, they do not change if the baseline is changed (Odum, 1996); (2) in general, results relative to any baseline can be converted into results relative to any other baseline by multiplying the transformities used by the appropriate conversion factor (Odum, 1996). However, they also pointed out reasons for concern, e.g., (1) the fact that several baselines exist in the published literature makes it very likely that transformities determined using different baselines will be combined in a study leading to errors in the results; (2) the role and importance of the planetary baseline and its effect on the transformities used in an emergy study was not well understood by many scientists using emergy methods at that time. Furthermore, the choice of the baseline itself can have a significant effect on the values determined for transformities when the baseline is adjusted to more accurately determine the emergy contribution to certain kinds of ecosystems such as coastal wetlands. For example, Lu et al. (2007) adjusted the transformities for river and rain water by removing tide from the emergy baseline for these inputs to avoid double counting them with the tidal input to an intertidal marine ecosystem dominated by *Spartina*, *Suaeda*, and mudflats. All baselines do not give the same number for the transformity of rain after it is adjusted to remove the tidal component, e.g., while the 9.26 baseline gives 15,724 sej J^{-1}, the value is 13,735 sej J^{-1} after making this adjustment from the 15.83 baseline, a difference of 14.5% in the adjusted value relative to the 9.26 baseline. These discrepancies and the importance of insuring uniformity in the results of emergy analyses prompted Campbell et al. (2010) to consider whether the planetary baseline is indeed arbitrary and to further examine the evidence to determine if there are reasons for preferring one baseline over another.

2.1.2. Critical examination of past baselines

Campbell et al. (2010) proposed two testable criteria for deciding among baselines: (1) The implications of any valid baseline with regard to the organizing power of the components of the baseline must be consistent with observations of the complexity of observed natural phenomena; and (2) baselines should conform to the principles of Energy Systems Theory or if not we should be able to explain why these principles no longer hold true. One EST principle that follows from the maximum empower principle (Odum, 1996) is that the fractional contributions of the emergy inputs to a system should represent the organizing power of those inputs over time periods long enough for the system to adapt to its available energy sources. Therefore; the complexity of the organization observed in a system should be found to be proportional to the emergy of the sources (inputs). The relative organizing powers of the primary emergy inflows to the Earth system are indicated by their relative contributions to the total emergy of the baseline. Table 1 gives the expected relative organizing power of the various possible configurations of the inputs, thus far used to establish the equivalences between solar radiation and deep Earth heat and solar radiation and the energy of the tides. This table has been modified from Campbell et al. (2010) to include the baseline of Brown and Ulgiati (2010).

A second principle of EST that can be used to judge the validity of a baseline is the principle of energy quality matching, i.e., the maximum empower principle (Odum, 1996) indicates that higher quality (higher transformity) energy flows will be matched with lower quality (lower transformity) energy flows to create flows of intermediate quality. Over the long run, this principle should lead to both high and low transformity inputs contributing approximately equal quantities of emergy (i.e., organizing power) to the emergy of the output of the interaction and by extension to the system as a whole[7], thereby maximizing the empower gained from all inputs. The numbers underlined and in red in Table 1 indicate that the energy quality matching in these configurations is inefficient compared to other possible configurations.

[7] The emergy matching principle has similarities to Liebig's law of the minimum in that when the emergy contributed by both the low and high transformity inputs to a process is the same neither input is limiting and the process operates close to the optimum efficiency for maximum empower (Odum, 1996, p. 165).

If these two criteria are valid, we have a method for testing the validity of any baseline by determining the complexity of the organization of structural phenomena on maps, where the observed organization is primarily caused by one of the three independent inputs to the baseline. The results of this analysis can then be examined to see if the complexity measured is implied by the relative proportions of organizing power (emergy) in the baseline.

2.1.3. Calculation of the planetary baseline using the exergy of S, E, and G

Brown and Ulgiati (2010) updated the value of the 15.83×10^{24} seJ y^{-1} planetary baseline (Odum, 2000) by expressing the energy inflows to the Earth's geobiosphere in terms of available energy or exergy and by using more complete or more accurate estimates for the tidal and geothermal energy inflows, respectively. They also reinterpreted the interaction of the Earth's geothermal energy sources driving geobiosphere processes such that the radiogenic energy sources in the crust were grouped with "crustal heat", i.e., heat that was, in part, assumed to be of solar origin, instead of with the deeper sources of Earth heat. They stated that this regrouping was necessary to apply different Carnot efficiencies (Table A4, note "d") to the various heat flows, which Odum did not include in his calculations. They used a system of two equations and two unknowns to solve for the solar transformities of crustal exergy flow and the tidal exergy inflow following Odum (2000). In both cases, the values of the various available energy inputs to the equations are based on different data or manipulations of the data compared to those used by Odum (2000). Specifically, the equation used to solve for the transformity of "crustal heat" was restructured to separate the heat from radioactive decay from other "crustal" sources. The structure of the second equation used to calculate the transformity of the tides separates Odum's category "deep Earth emergy" into heat from radioactive decay and deep heat from the Earth's core, because different Carnot ratios apply to each of these flows. They used a Monte Carlo analysis to characterize the uncertainty in global heat flows related primarily to the variability in estimates of residual heat flow from the Earth's core. Overall, Brown and Ulgiati (2010) took an important methodological step forward, because they made the calculation of the emergy baseline consistent with Odum (1996)'s definition of emergy in terms of available energy or exergy flows.

2.1.4. Alternative accounting methods

There are many possibilities for structuring accounting methods to trace the flows of available energy from their origins into the various products and services found in the geobiosphere, but so far these alternative accounting systems have not replicated the properties of Odum's original method. For example, Chen et al. (2010) propose a system of accounting based on cosmic exergy or the inflow of solar exergy to the Earth using the cosmic background radiation (CBR) as the temperature of the reference environment. However, their system does not recognize that the planetary exergy flows deriving from solar exergy are hierarchically organized and as a result they assign an equal portion of the exergy inflow from the sun to each of seven, second order planetary processes that they defined. The Earth's deep heat and the gravitational attraction of the Moon and Sun are not considered large enough to include in their system of accounting, thereby discounting the principle of energy quality. This approach allows accounting to be performed based only on the solar exergy input to the Earth, but the properties of emergy as a universal accounting quantity are lost.

Raugei (2013) proposed an alternative to the current methods and models (Odum, 2000; Campbell et al., 2010; Brown and Ulgiati, 2010) that use 2 equations to solve for 2 unknowns in calculating the equivalence between solar radiation and the available energy of the tides and between solar radiation and the available energy of the Earth's deep heat. He saw an epistemological problem in applying the emergy track-sum method to determine the planetary baseline, because the production functions for obtaining the exergy of the Earth's deep heat and the exergy of tidal dissipation from solar radiation are unknown. Raugei's solution to this problem was to use a "baseline vector", in which the three fundamental quasi-independent inputs to the Earth, (solar, tidal, and Earth heat exergy) were kept separate, and thus it is not necessary to determine their equivalences. In his proposal, an input of available energy to any product or service would be traced back to its origins in one of the three components of the baseline vector. While this method is epistemologically consistent with the track-sum method for calculating emergy, it has some significant disadvantages, not the least of which is that its adoption would require the recalculation of all transformities and their expression in a much more complex form, i.e., as a vector. Furthermore, the ability to express the value of all products and services in terms of a single unified unit, which is a fundamental advantage of environmental accounting using emergy, is lost in the process of making transformity a vector. However, Raugei's insight is incorporated in Brown and Ulgiati (2016) and in this paper through recognizing that emergy baselines for the Earth must be quantified as solar equivalent joules rather than as solar emjoules. While both Raugei's and Chen et al. 's approaches are thought-provoking, they both sacrifice fundamental properties of emergy accounting. Thus, they are not viable solutions to the baseline question within the context of the evaluation methods proposed by Odum (1996).

2.2. Reasons for recalculating the emergy baseline of the Earth at this time

There are three reasons that make it necessary for us to recalculate the emergy baseline of the Earth at this time. The first is that there have been recent advances in our understanding of the Earth's geophysics (i.e., the view that the Earth formed as a cold body with subsequent core differentiation, Sorokhtin et al., 2011). This model provides a viable alternative to the currently accepted model of Earth's evolution (i.e., the view that the Earth formed as a hot body with current residual heat flux from the core), which has been used in all prior calculations of the planetary baseline. The second is that the Earth's energy budget (Sclater et al., 1980) as translated by Odum and Odum (1983), and as used to some degree in all subsequent studies of the emergy baseline to date, contains an error that makes the proposed model used to calculate the transformity of "crustal" heat flow inconsistent with the geophysical data on the Earth's heat fluxes. Third, the model used by Odum (2000) to calculate the equivalence between solar energy and tidal geopotential energy is formulated unrealistically in that it was assumed that all three sources of available energy inflow (S, E, and G) are coupled in a mutually necessary multiplicative interaction on the time scale of one year, which implies that the available energy contributions from all three inputs will have a significant effect on the output variable, the geopotential energy of the ocean. In other words, the changes caused by the annual variations of the variables are expected to be within the same order of magnitude on the timescale of the calculation. In addition, the relationship between solar energy and the Earth's deep heat flow used in these models incorrectly assumes that the gravitational forces of the Moon and Sun play a substantive role in determining the deep heat flow from the Earth. The evidence supporting the need for calculating a new emergy baseline for the Earth is examined in more detail in this section

2.2.1. An alternative theory of the evolution of the Earth

A considerable amount of uncertainty exists with regard to the current heat budget of the Earth (Anderson, 2005; Mareschal et al., 2012). This uncertainty has centered on finding and quantifying heat sources with enough heat flow to balance the observed total heat loss from the Earth's surface. These sources are the decay of radioactive elements in the Earth's crust and mantle, secular cooling of the Earth's mantle, and heat flux from the core (Mareschal et al., 2012). Residual heat flux from the core implies a hot origin for the Earth, which is the dominate paradigm of the Earth's formation used by many geophysicists today.

Recently, a group of Russian scientists (Sorokhtin et al., 2011) have published a comprehensive treatise on the evolution of the Earth. Drawing on the earlier proposals of Schmidt (1946) and Runcorn (1962, 1965), Sorokhtin et al. (2011) make a convincing argument for a cold origin of the Earth based on one physical concept and two assumptions. The physical concept, which has been thoroughly reviewed (Wetherill, 1990), is that the Earth was formed approximately 4.6 billion years ago as the result of the homogenous accretion of a gas and dust cloud, the proto planet (Schmidt, 1958; Safronov, 1969). The first assumption is that the young Earth had a uniform composition with neither a dense core nor a light crust. To support their hypothesis that the young Earth was a cold body, they cite evidence that the oldest rocks found on Earth are 600 to 800 million years younger that the probable age of the Earth. Since relatively high temperatures and melting are required for rock formation, this implies that the Earth was a cold body for the first 600 to 800 million y. In contrast, the oldest igneous rocks from the lunar crust are 4.6 to 4.4 billion years old, which is evidence that the interior of the moon was originally in a hot or melted state. The second assumption follows from the fact that the chemical composition of the primordial Earth would have determined its endogenous potential energy. In this regard, Sorokhtin et al. (1971) proposed that the outer core of the Earth is now composed of a eutectic alloy of iron and iron oxide, i.e., the oxide of univalent iron, and the inner core is composed of an iron-nickel alloy. Under these conditions, they determined that the primordial Earth would have been composed of about 13% free (metallic) iron and 22–24% bivalent iron oxide distributed throughout the Earth's original mass. Sorokhtin et al. (2011) observe that thermodynamic principles dictate that the largest contributions to the Earth's evolution will be from processes that lower to the minimum the internal potential energy of the Earth and of the Earth–Moon system as a whole. They further observe that the heat released from these processes is eventually lost to outer space and thus the evolution of the Earth and of the Earth–Moon system is irreversible. Under this geologic scenario, the main planetary process controlling the evolution of the Earth will be the chemical-density differentiation of the Earth's original homogenously distributed matter. According to Sorokhtin (1974), this process along with a close encounter with the Moon at or near the Roche limit[8], which generated enough heat to melt iron and begin the initial separation and growth of a dense iron oxide core and the development of chemical-density driven circulation (i.e., convection) in Earth's silicate shell (i.e., the mantle). For more details on the mechanisms and progress of core formation see Sorokhtin et al. (2011).

Following this theory, at present, 90% of the endogenous energy released from the Earth can be accounted for by chemical-density differentiation, a little less than 10% by the decay of the remaining radioactive elements and about 1% from tidal deformations of the Earth's body. The ability of the cold body model to generate sufficient heat to account for current heat losses is in contrast to the aforementioned problems in finding sufficient heat sources to account for current losses using the hot body model.

2.2.2. Errors in and clarifications of the existing calculations

Several improvements in the calculation methods have been made over the course of the evolution of scientific thought on the baseline, as recounted above. While the numbers and models used in the calculations have been examined and modified by Brown and Ulgiati (2010), remaining conceptual and factual errors will be elucidated in this section.

2.2.2.1. Clarifications and errors in the calculation of the transformity of the tides. Brown and Ulgiati (2010) updated the information on tides used in the baseline calculation based on Munk and Wunsch (1998), but some clarifications are still needed based on their interpretation of the data. First, there is no increase in measurement accuracy between the numbers reported by Munk and Macdonald (1960) and used by Odum (1996) and those reported by Munk and Wunsch (1998), since the energy supplied by the major semidiurnal lunar component, M_2, is the same in all cases. It was not better measurement methods, but rather an expansion of the estimate to make it more comprehensive that was the main reason for the larger number for the total tidal energy dissipated in Munk and Wunsch (1998) compared to Odum (1996).

Furthermore, Odum (1996) used data from Miller (1966), who estimated a value of 1.7 TW (1.65 TW in Odum) for the total dissipation of lunar tidal energy in shallow seas. Odum assumed that this was the available energy required for generating tidal currents in the shallow seas, and thus he could apply a transformity for currents in the Mississippi River mouth as a surrogate for tidal currents in determining the planetary baseline as described above. In this study, the tidal energy dissipated in the world oceans (3.5 TW) is the portion of the total tidal energy flux (3.7 TW) that is directly related to the creation of the geopotential energy of the oceans (Munk and Wunsch, 1998). This number is different from Brown and Ulgiati (2010) who used the total tidal energy dissipation for the whole Earth, i.e., including the Earth tide (3.7 TW). The total tidal energy dissipation estimate of Munk and Wunsch (1998) is 124% (3.7 TW/1.65 TW) greater than that used by Odum (1996).

Two additional problems with the information used to calculate the solar transformity of the tides in past studies are related to the original number for the geopotential energy of the world oceans taken from Oort et al. (1989) and its use in Campbell (1998) and in subsequent calculations of the baseline. First, this number is a stock of available energy and not a flow, and thus a turnover time must be applied to calculate the annual flow of available energy. This fact was recognized by Campbell (1998) and Odum (2000) and in their work the turnover time was assumed to be 1 year. Oort et al. (1994) give enough information to make an estimate of the turnover time of the geopotential energy in the world oceans. Second, the numbers given in Oort et al. (1989) refer to the oceanic geopotential energy generated in a world with ice-free polar oceans rather than in the ice-covered oceans present today and the analysis only quantifies the solar generated geopotential energy of the oceans, thus areal extent of stratification in the world oceans must be corrected and the geopotential of the tidal energy added to the estimates in Oort et al. (1989) to estimate the total geopotential energy generated and dissipated annually in the world oceans, which is not the formulation used in past calculations. These relationships are confirmed in a later paper (Oort et al., 1994) from which the numbers used in this paper are drawn.

2.2.2.2. Errors in prior calculations of the solar transformity of crustal heat. There is a substantial error in Odum and Odum's (1983) calculation of the energy budget of the Earth, which has been

[8] The Roche limit is the minimum distance to which a satellite can approach its primary body without disintegrating due to the gravitational forces of the larger body overcoming its own cohesive forces.

perpetuated to some degree in all subsequent calculations. This error resulted from a misinterpretation of Sclater et al. (1980) and it led to a conceptual and a numerical error in the calculation of the solar equivalence of the deep Earth heat flow. In the abstract of Sclater et al. (1980, p. 294), the total heat loss from the Earth is given as 42 TW (41.94 TW) based on a total heat loss from the surface of the Earth of 1002×10^{10} cal s^{-1}, which was divided into three components: heat loss from convective processes, conduction through the lithosphere, and radioactive decay within the continental crust. Sclater et al. (1980) attribute about 2/3 of the heat loss to convection assuming that 1/2 of the heat flow from the youngest crust derives from magmatic activity. However, this convective loss was not considered in the heat budget constructed by Odum and Odum (1983); instead this loss was attributed to heat generated from various inputs of solar origin, e.g., the work of rain, wind and sun in eroding the Earth's surface, the burial and compression of sediments with their chemical potentials.

Odum and Odum (1983) calculated the conductive heat loss from data in Sclater et al. (1980) by averaging the range of heat flows for the continents ($0.4–0.75 \times 10^{-6}$ cal m^{-2} s^{-1}) and the oceans ($0.6–0.9 \times 10^{-6}$ cal m^{-2} s^{-1}) and prorating by the area, assigning 71% to the oceans and 29% to the continents, assuming 3.154×10^{7} s y^{-1}, 5.14×10^{14} m^2 for the area of the Earth and 4.186 J cal^{-1} to give 4.744×10^{20} J y^{-1} for the global heat loss from conduction[9]. Although this number was for conduction only, Odum and Odum (1983) assumed that it was the total contribution of the mantle to heat loss (i.e., conduction plus convection). The number for total heat flow is accurate based on total heat loss reported by Sclater et al. (1980), but given 4.186 J cal^{-1} and 3.154×10^{7} s y^{-1}, the number should be 13.23×10^{20} J y^{-1} instead of 13.21×10^{20} J y^{-1}. The number for radioactive heat production in the crust, 1.98×10^{20} J y^{-1} or 15% of the total heat loss is the same as in Sclater et al. (1980). The remaining heat flow, 6.49×10^{20} J y^{-1} or 49% of the total heat loss, using Odum's uncorrected number is within the margin of error for these calculations. For example, if the minimum value for conductive heat flow from the continents is used, i.e., 0.6×10^{-6} cal m^{-2} s^{-1}; convective processes account for 2/3 of the total heat loss (Sclater et al., 1980). The "missing" heat flow, 6.49×10^{20} J y^{-1}, was attributed by Odum and Odum (1983) to the work of solar energy on the Earth's surface, instead of to convective processes as intended by Sclater et al. (1980) and this error has been passed forward in all subsequent calculations up to Brown and Ulgiati (2010)'s reexamination of the Earth's heat budget and reformulation of the equations to apply Carnot ratios to the different sources of heat. Even though Brown and Ulgiati (2010) reformulated the two equations used by Odum (2000) and redefined and added uncertainty bounds to the sources of heat, they did not discuss the underlying error in Odum's original calculation.

It is easy to verify that attributing such a large available energy flow (6.51×10^{20} J y^{-1} using the corrected value) to erosive processes and the burial of organic matter from the Earth's surface must be an error, since the available energy dissipated by erosion of the continents is on the order of 10^{17} J y^{-1} (Wilkinson and McElroy, 2006) and around 0.1 Gt of carbon is buried in the world oceans each year http://soilcarboncenter.k-state.edu/carbcycle.html or 5×10^{18} J y^{-1} assuming carbon is 50% of dry weight, dry weight contains 5 kcal per g and that there are 4186 J $kcal^{-1}$ http://nefsc.noaa.gov/publications/crd/crd0615/pdfs/2.pdf. Thus, solar energy sources can account for less than 1% of the energy needed to balance the Earth's heat budget in this quick calculation. Since both the model and the data used to establish equivalence between the Earth's heat flow and solar energy are inconsistent with what is known of the Earth's heat budget and the operation of geological processes, clearly a new calculation of the planetary baseline is warranted, if only for the sake of increasing the accuracy of the estimate.

2.2.3. Characteristics and applicability of the models used to determine the equivalences

Since it has been demonstrated that a new calculation of the emergy baseline is warranted based on errors in data translation and interpretation, the pros and cons of the models that have been used to establish these equivalences are now considered. In the original calculations (Model 1) of Odum and Odum (1983), the equivalence between solar radiation and the deep heat flow from the Earth relied on establishing the fraction of the total deep heat flow generated by the work of solar energy on the Earth's surface by taking the difference between estimates of the heat flow generated by processes within the Earth and the total heat outflow at the surface. Once this value was obtained the solar transformity of the solar fraction of the total Earth heat flow could be calculated and then a transformity for the remaining Earth heat flow imputed by the transitive property of equalities, assuming that all Earth heat flow is equivalent regardless of its origin. This is an elegant method, but the actual calculation was marred by errors in the magnitude of the solar derived flows and in the interpretation of the Earth's heat budget as pointed out above.

In applying the solar equivalent energy baseline of the Earth as the basis upon which all calculations of transformities of emergy flows on the planet can be made, the Earth's geobiosphere and its subsystems, e.g., atmosphere, oceans, crust, are considered to be one system composed of mutually necessary, coupled sectors (Odum, 1996, Fig. 3.2). In this view, the Earth can be represented as an interaction of closed loops in which each component interacts with the others and each flow in the aggregated system is a by-product of the other interacting flows (i.e., the outputs of each sector are co-products). In such a system all of the solar equivalent energy flowing into the system is required for all of the flows within the system. The total inflowing to the geobiosphere is that carried by the available energy of solar radiation, the gravitational attraction of the Moon and Sun and the heat flow from within the Earth. This logic is used by Odum (1996) to relate all secondary, tertiary, and higher flows of available energy on Earth to their base in the three primary planetary inputs.

Odum (2000) used this logic in structuring (Model 2), the system of two equations and two unknowns that he used to solve for the equivalence between solar radiation and tidal energy and between solar radiation and the deep heat flowing from the Earth. While this method is mathematically eloquent and draws upon the eigenvalue method of determining transformities (Collins and Odum, 2000), it is now apparent that these models are too highly aggregated in time to accurately reflect the Earth processes responsible for generating the annual production of a particular product, e.g., plate movements or the annual elevation of the ocean surface.

Over long time scales, at a high level of aggregation, an argument can be made that coupled multiplicative interactions of all geobiosphere components will develop, i.e., the Earth system will be composed of a completely coupled, mutually necessary set of components. However, such close multiplicative coupling among all of the inflows of available energy often is not observed, when

[9] For the sake of accuracy, we observe that Odum and Odum (1983) report on page 379 that they used 0.6×10^{-6} cal m^{-2} s^{-1}, for the heat flow from the mantle to the crust, but the actual number used in the calculation was the average mentioned in the text, 0.69925 cal m^{-2} s^{-1}. Such minor errors often appear in pioneering work and are to be expected; however, the baseline is used in a relativistic manner in emergy evaluations. Thus, the value of having an approximate, agreed-upon baseline far outweighs minor errors made in determining the baseline's exact value.

the details of a particular physical process or annual production function are considered (Model 3). For example, both the net effect of heating and fresh water inflow cause a decrease in the density of ocean surface waters and these two effects, both of which result in an elevated water surface, are additive. Multiplicative effects may also occur, such as the interaction of wind and storms in delivering freshwater inflows to the ocean surface and some inputs such as heating have both positive, e.g., stearic expansion, and negative, e.g., the loss of water through evaporation causing an increase in salinity and density, effects on surface water density (Wijesekera and Boyd, 2001). Similarly, the gravitational pull of the Moon and Sun causes the level of the sea to rise and fall, thereby creating geopotential energy in the world oceans that adds to that created by solar heating and fresh water inflow. In contrast, the heat flow through the ocean bottom is about 0.001 that of the input from the sun, and it heats the entire water column from the bottom up, raising the entire mass of the ocean a tiny amount through bulk heating, but adding nothing to the annual creation of geopotential of the oceans.

Completely connected models (Model 2) like the one shown in Odum (1996) and in Brown and Ulgiati (2010) represent the Earth at a high level of aggregation that may exist on long time scales. For example, if the time scale of the geopotential energy evaluation is extended to a period of 10 million years; thereby allowing for a movement of about 500 km in the position of the continents at the rate of 5 cm of continental drift in a year (Conrad and Lithgow-Bertelloni, 2007), the resonant frequencies of the global tidal harmonics may change either increasing or decreasing the efficiency of the configuration of the Earth's continents in producing tidal energy (Kagan, 1997). Such changes in the configuration of the continents are thought to be cyclical (Sorokhtin et al., 2011); however, the efficacy of the continents in producing tidal emergy is effectively constant on time scales of 10,000 years or less (movement of <0.5 km) and thus the movement of the continents would be negligible (~0.00005 km) over an annual cycle of the creation of geopotential energy in the oceans. However, over the history of the Earth, since the formation of the world's oceans, the gravitational attraction of the Moon and Sun has produced large changes in the generation of geopotential energy in the world oceans due to the changing tidal harmonics on the Earth' surface. In addition, the Moon may have played an indispensable role in the generation of Earth heat flow by initiating formation of the Earth's core through the gravitational energy dissipated as heat in a close encounter of the Moon with the Earth near the Roche limit (Sorokhtin et al., 2011).

On geologic times scales, a completely coupled model (Model 2) with mutually necessary inputs may be a valid model of the interaction of solar, tidal, and deep heat flow driving the geobiosphere; however, the interaction of the forces driving annual production processes is not well represented by the slowly changing forces operating in completely coupled multiplicative formulations. In Table 1, both the models using a completely coupled system give inconsistent results. Brown and Ulgiati's model shows that the tide is twice as important as the sun in the emergy base of the Earth; whereas, Odum's model indicates that the Earth heat flow is twice as important as the sun and the tide. Both models using only two elements to evaluate the tidal emergy found that tides contribute about a third of the emergy that the sun and the Earth heat flow contribute, which is similar to the result found by Odum (1996) for the 9.44 baseline. The final formulation with S, G and E contributing to the generation of oceanic geopotential energy shows that tidal energy is about 2/3 as important as the sun and Earth heat, but as argued above this formulation is not physically reasonable for the generation of geopotential over a year. Therefore, all models formulated using the "two equations and two unknowns" method appear to give unreasonable or inconsistent results. For this reason, in this study, the calculation method has been simplified to apply the transitive property of equalities to evaluate single physical processes to which two of Earth's independent exergy sources contribute in a physically meaningful way and for which such equivalences can be calculated, at least as a reasonable first order approximation.

Nevertheless, the assumption that the Earth's geobiosphere is a completely connected system is still valid, when viewed over the long run, i.e., over a time period sufficient for the Earth system as a whole to adapt to changes in its exergy inflows. Even in the short run, all three quasi-independent inputs of solar equivalent energy to the Earth are directly or indirectly coupled to all the others, although the coupling is not always multiplicative on the annual time scale, e.g., Odum (1978) shows a more detailed model of the global geobiosphere with additive as well as multiplicative interactions among the flows and processes. Thus, from this perspective, the entire baseline is required for the system that produces any product or service on the scale of the entire planet. For this reason, the planetary baseline effectively represents the solar equivalent joules required for Earth's secondary (e.g., rain and wind) available energy flows and these, in turn, are concentrated into the tertiary available energy flows (e.g., waves, currents, etc.) that are expressed as emergy flows (sej y^{-1}).

3. Methods

In this paper, detailed models of two Earth processes are used to calculate the equivalences between the exergy of solar radiation and the exergy of the Earth's deep heat and between the exergy of solar radiation and the available energy dissipated from the tidal geopotential energy of the oceans. This study follows Brown and Ulgiati (2010) in quantifying the exergy driving processes within the Earth system (i.e., the geobiosphere). However, different choices have been made with regard to certain boundary conditions. For example, the exergy of an input to the Earth, e.g., solar radiation, is a function of the ground or background state chosen for the calculation. In this paper, the temperature of the cosmic background radiation (CBR) outside the Earth's atmosphere is the temperature of the background state against which the order and organization of the Earth system as a whole are created (Chen, 2005), whereas Brown and Ulgiati (2010) used the surface temperature of the Earth.

This study relies on Sorokhtin et al. (2011) for much of the background data needed to make the historical calculations presented in this paper. As discussed above, Sorokhtin et al. (2011) present a cold body approach to explaining the evolution of the Earth that differs from the currently accepted theory in the West, the hot body theory (see Section 2.2.1). However, the cold body theory is able to account for some deficiencies in the explanatory power of the hot body theory and Sorokhtin et al. (2011) support their theory with many calculations and cite supporting empirical evidence in a compelling manner. They also include a detailed record of almost all of the variables needed to calculate the components of the planetary baseline over the periods of the Earth's history examined in this paper. Because data from Sorokhtin et al. (2011) were used for the historical analysis (see Appendix A) and averaged data from contemporary studies of the Earth's heat budget and from other sources were used to evaluate present Earth processes (see data in the tables presented in the text), there will be some differences in the numbers presented for the same processes in the historic and contemporary analyses. Therefore, one cannot make an exact comparison between the two analyses. The reader should note that energy data will be presented both as terawatts (TW) and as joules (J) as appropriate to past and present descriptions of the data. Terawatts can be converted to joules per year by multiplying by 1.0×10^{12} J TW^{-1} and then by 3.1557×10^{7} s y^{-1}.

3.1. Emergy methods and modifications

The methods used in this study follow the guidelines in Odum (1996) for emergy evaluations and draw on the principles of EST described in Odum (1994). However, the track-sum method commonly used for determining the emergy of a quantity was not applied to the problem of establishing an emergy baseline for the Earth, because the production functions for the three quasi-independent inputs of available energy to the Earth system were not known. Thus, it was not possible, given our current state of knowledge, to employ the usual method of tracking and summing all necessary inputs of available energy to calculate the solar transformity of the available energy flows generated by deep Earth heat and the gravitational attraction of the Moon and Sun. However, the principles of logic can be employed to estimate these relationships (Odum and Odum, 1983 and above). The difficult accounting problem of establishing equivalences between the three quasi-independent available energy inflows to the Earth can be circumvented by applying one of the oldest principles of logic —the transitive property of equalities, or Euclid's Axiom, i.e., two things equal to a third thing are equal to each other. To apply this method, it is necessary to first choose two real processes to which both solar radiation and one or more of the other primary inputs contribute in making something that is effectively the same product.

3.2. Energy systems language models

The first step in performing an emergy evaluation is to construct an Energy Systems Language (ESL) diagram (Odum, 1971, 1994) of the system or systems of concern. The ESL model gives a conceptual overview of what is required to answer the address the problem or answer the question of concern. Therefore, the following two questions: "What is the equivalence between solar exergy and the exergy of deep heat flow from the Earth?" and "What is the equivalence between solar exergy and the geopotential exergy dissipated in the world oceans?" were answered by constructing ESL models of the Earth systems responsible for generating the tectonic activity of the Earth and the geopotential energy of the world oceans.

3.2.1. ESL model to evaluate the generation of geopotential energy in the world oceans

To evaluate the global processes creating the geopotential energy of the world oceans, first, the ocean geopotential energy is assumed to be the same regardless of how it is created. i.e., oceanic geopotential energy is the same regardless of its source. Thus, the geopotential energy of the world oceans generated by solar exergy was considered to be identical with the geopotential energy of the world oceans generated by the gravitational attraction of the Moon and Sun in terms of the potential to do work, despite the fact that the generation processes are different and different work might be done by the different sources. The exergy of the tides is the same as the gravitational potential energy generated by the height difference between high and low tide over a year (Brown and Ulgiati, 2010; Hermann, 2006). The exergy of the solar part of the geopotential energy of the world oceans was calculated in Oort et al. (1989), who chose the equipotential surface at the mean ocean depth of −3750 m as the reference level (Oort et al., 1989)[10].

Next, an ESL diagram of the system generating geopotential exergy in the world oceans is drawn (Fig. 1). In this model solar exergy, S, and the exergy of the tides, G, interact to create the total geopotential of the world oceans over a year. In the model,

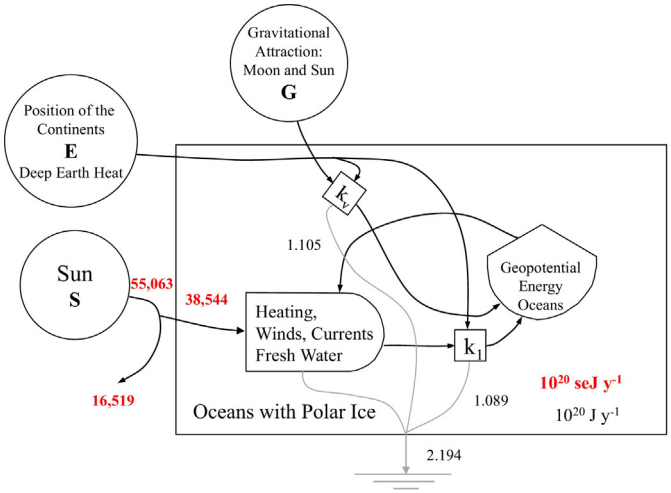

Fig. 1. Energy Systems Language (ESL) models of the generation of the geopotential energy of the world oceans. (A) The present world with ice-covered, polar oceans; (B) The world prior to 3.4×10^7 BP without ice-covered, polar oceans (see Table A1 and Fig. 4). ESL symbols from Odum (1994) are defined as follows: Circles are sources of emergy, bullet symbol is a production function, tank is a storage of potential energy, large box represents the system boundaries, and the small boxes are the sites of available energy dissipation, which leaves through the bottom of symbols (i.e., the gray lines going to the heat sink or ground symbol). Numbers in red bold text are emergy and the numbers in black plain text are available energy. (For interpretation of the references to color in this figure legend, the reader is referred to the web version of this article.)

the amount of geopotential exergy generated by the sun and tides is also a function of the exergy driving plate tectonics, E, over 10^6–10^7 y, i.e., a 50 to 500 km translation in the position of the continents for an average rate of movement of 5 cm y^{-1} (Conrad and Lithgow-Bertelloni, 2007). For example, the amount of geopotential energy of the oceans generated from solar exergy was larger in the past, when the world was without ice-covered polar oceans (Oort et al., 1994). Antarctic ice sheets had developed by 34,000,000 y BP

[10] Note that the geopotential energy of the world oceans is the same as the geopotential exergy of the world oceans, since both are measured relative to the same ground state.

with small ephemeral ice sheets forming as early as 37,000,000 y BP (Zachos et al., 2001). For this reason, the model for the generation of the solar portion of the ocean geopotential exergy is divided into two states, one for a world with ice-covered polar oceans (Fig. 1A), which was assumed to be present from 34,000,000 y BP to the present and a second without ice-covered polar oceans (Fig. 1B), which applies to the Earth prior to 34,000,000 y BP. These two global states are represented in Fig. 1A and B, respectively, by two constant coefficients, k_1, representing the geopotential energy created in a global ocean with polar ice, and k_2, for an ocean without ice-covered polar oceans. In addition, the model in Fig. 1 includes a variable coefficient, k_v, which only varies meaningfully over very long time periods, e.g., 10^6–10^7 y. This coefficient represents the slowly changing position of the continental land masses that results in a slow change in the tidal resonance properties of the configuration of the land masses on the surface of the Earth (Kagan and Maslova, 1994). These slow gradual changes in the position of the continents can result in a decrease or an increase in the tidal exergy generated based on the effects of the configuration of the continents on the tidal resonance properties of the system (Kagan, 1997). Both the movements of the continents and the opening and closing of polar oceans are largely controlled by the deep Earth exergy flows driving plate tectonics as represented by E in Fig. 1.

The models in Fig. 1 were evaluated based on studies of the geopotential energy dissipated annually from solar sources[11] (Oort et al., 1989, 1994) and from data on the tidal energy dissipated in the world oceans (Munk and Wunsch, 1998). The transitive property of equalities (if $a = b$ and $b = c$; then $a = c$) was applied by taking the ratio between the solar exergy absorbed on the Earth's surface and the ocean geopotential exergy generated from solar sources and dissipated annually. The solar transformity of the geopotential exergy generated from solar exergy and dissipated annually in the world oceans (a) was determined from Oort et al. (1989, 1994). Assuming that the geopotential exergy dissipated in the world oceans (b) is the same regardless of source, so that the transformity of the oceanic geopotential is the same as that of the solar part of the total ($a = b$). In addition, the gravitational attraction of the Moon and Sun also forms oceanic geopotential energy that is dissipated annually by the tides and has transformity ($c = b$). The transitive property of equalities can be applied to establish equivalence between solar exergy and tidal exergy. Note that the solar transformity of the tidal geopotential exergy dissipated in the world oceans (c) is effectively equal to the solar transformity of the solar generated geopotential exergy dissipated in the world oceans (a) because both are equal to the transformity of geopotential energy in the oceans (b), i.e., $a = b$, $c = b$, therefore $a = c$).

3.2.2. ESL model to evaluate the Earth cycle

A second global process, the Earth Cycle[12] was chosen for evaluation to determine the equivalence between solar exergy and the exergy of deep heat flow from within the Earth, i.e., specifically the heat flow from within the Earth responsible for tectonic processes moving the crustal plates (Sorokhtin et al., 2011) and also supporting isostatic adjustment of the continents through buoyancy mechanisms. Fig. 2 shows a model of the Earth Cycle, which is driven by the heat gradient between the mantle and the crust and by the operation of solar exergy on the Earth's surface as heating and cooling and through the hydrologic cycle. The symbols on Fig. 2 identifying the forcing functions (circles), components (tanks and the bullet symbol) and pathway flows (lines ending in arrowheads) are defined in Table 2 and in the caption of Fig. 2. The forcing functions include solar exergy operating on the surface of the Earth (S), the exergy of the gravitational attraction of the Moon and Sun (G) and exergy of the heat flow from deep within the Earth dissipated in uplift from isostatic processes and plate movements (pathway flows h_3 and h_4, respectively). Components in the model include the Earth's mass divided into four major compartments: oceanic (OC) and continental (CC) crust, the mantle (M), and the core (C). Storages of the remaining mass of radioactive elements (the R_i's) and heat (the H_i's) are shown within each of the 4 compartments. The remaining gravity-chemical potential energy (GC_M) stored in the mantle (Sorokhtin et al., 2011) is shown along with the flows of used energy going to the heat sink, the h_i's. The gradient between the average temperature of the mantle (T_M) and the temperature of the crust at the ocean bottom (T_{OC}) defines the heat gradient driving plate tectonic processes and multiplying the resulting Carnot ratio by the deep Earth heat flow driving plate movements gives the exergy dissipated to drive uplift caused by both plate movement and isostatic processes ($h_3 + h_4$)[13]. Gravitational attraction, G, acting as the Earth tide is a "body" force that increases heat in all compartments, but does not contribute to the heat gradient, *per se*. The dissipation of the exergy of the ocean tide is not shown here, but since it supplies heat at the surface of the Earth, it will not increase the heat gradient driving tectonic processes, i.e., ∇H, where H is the heat field driving convection.

This evaluation of the solar equivalence of the exergy of deep Earth heat relies on the underlying assumption that over geologic time the rates of all uplifting tectonic processes, including uplift to maintain isostatic equilibrium and uplift by mountain-building, must be balanced by erosional losses (Wilkinson and McElroy, 2006; Verhoogen, 1980). The fact that the average elevation of the continents has been stable over the past billion years (Sorokhtin et al., 2011) indicates that this is a reasonable assumption. On one hand, the energy dissipated in erosional losses is fairly easy to calculate, since the energy released is simply that of a mass m, falling through a distance, h, under the acceleration of gravity, g, so the potential energy dissipated is $U = gmh$. On the other hand, the total work against gravity required to raise a body of sedimentary rocks from below sea level to the average height of a mountain range and to displace a sufficient amount of heavier mantle rock to serve as the mountain's root is more difficult to determine without detailed information on the density structure of the mantle and crust before and after the event (Verhoogen, 1980). To avoid this difficult calculation, the energy dissipated in uplift is assumed to balance the energy dissipated in erosion over long time periods.

To avoid the confounding effects of agricultural erosion on the estimate of the long term condition of the Earth Cycle, the value used for the continental mass eroded in the present time was estimated from the sediments carried to the sea by large rivers during the Pleistocene (Wilkinson and McElroy, 2006). In this case, a variation of Euclid's principle is used to estimate the solar transformity of the exergy of deep Earth heat exergy dissipated in driving tectonic processes by first calculating the solar equivalent energy of the available energy dissipated by land erosion (a) and noting that the available energy dissipated in annual land erosion (b) is equal to the available energy of the Earth's deep heat driving the tectonic

[11] Density is lowered by the effects of solar heating on the surface waters and by fresh water inflows from continental runoff and rain, thus creating the solar portion of the oceanic geopotential energy.

[12] In Odum (1996), Earth Cycle refers to the cycle of erosion and isostatic adjustment without change in elevation. In contrast, uplift and subsidence are driven by plate movements colliding with continents and by subduction of plates beneath them. In this paper, we use the term "Earth Cycle" to refer to both processes, because The Earth's heat or "deep" heat gradient contributes to driving convective flows to move plates and to the heat needed to support the mantle density, which determines the buoyant uplift balancing erosion.

[13] By assumption, all of the heat flow driving tectonic processes is required for the uplift caused by plate motion and isostatic adjustment, even though other processes may be driven by the same heat flow.

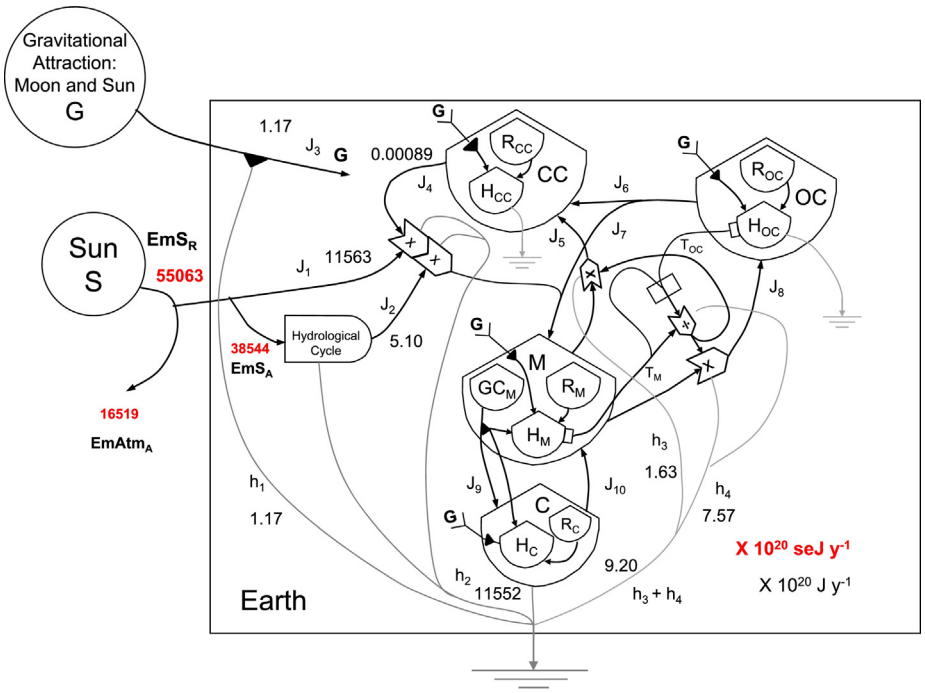

Fig. 2. Energy Systems Language (ESL) model of solar energy and deep Earth heat flows driving the tectonic processes of the Earth Cycle. See Table 2 for definitions of the model components and pathways (e.g., $h_3 + h_4$ is the heat driving isostatic and tectonic processes from Table 7, note b). In this figure, "eeJ" stands for Earth heat equivalent joule. The pointed arrows are interaction symbols, for multiplication and division (Odum, 1994); converging flows are addition; the Carnot ratio is represented by the configuration, $(T_M - T_{OC})/T_M$. Model components are CC, continental crust, OC, oceanic crust, *M*, mantle, *C*, Earth's core. *R* designates storage of radioactive elements and *H* storage of heat within a component. The black triangles indicate that a dissipative process generating heat is occurring on the pathway. Numbers in red are emergy and the numbers in black are available energy flows.

process with respect to the equivalence of the work done in the Earth Cycle, i.e., exergy dissipated in eroding a mass is assumed to be equal to the exergy dissipated in uplifting an equivalent mass. In this case, the solar transformity of the work of erosion (a/b) is equal in effect to the Earth heat equivalence of the work of uplift (c/b). Then the solar emergy equivalence of Earth heat equivalent joules (eeJ) is given by (a/c), where the available energies of uplift and erosion cancel to give the solar equivalent energy per unit of available energy in deep Earth heat flow (seJ J^{-1}). To make this calculation possible, the processes of erosion and uplift are assumed to be separable and solar exergy is assumed to be entirely responsible for erosion and the Earth's deep heat flow (i.e., the total heat flow supporting plate tectonics and isostasy) is entirely responsible for uplift. These two assumptions may be plausible for a 1st order analysis, even though the two processes are coupled.

3.2.3. Calculation of the emergy baseline of the Earth

Once the solar transformities for the tidal exergy dissipated in the world oceans and exergy of deep heat flow driving the Earth Cycle are determined, the planetary baseline of the Earth can be calculated by multiplying the values of the solar transformities of sun, tide, and deep Earth heat by the appropriate values for the solar, tidal and deep heat exergy flows received by the geobiosphere, annually, which were determined by evaluating the models shown in Figs. 1 and 2 (see Section 4).

3.3. Methods for historical reconstruction of the planetary baseline

Because of the importance of the planetary baseline and the need to decrease uncertainty with regard to its value, searches were performed for studies that would allow construction of the emergy baseline of the Earth over a long period of time to better understand its variability. To obtain estimates of the solar transformity of the exergy of the ocean tides and tectonic processes of the Earth, the same models and methods that were used above to determine the present values of the exergy flows and their equivalences were used to find the past equivalences between solar exergy and the exergy of the ocean tides and Earth deep heat flow. The methods used to determine the historical inflows of solar radiation, the Earth's deep heat, and tidal geopotential energy follow.

3.3.1. Method of estimating solar radiation over time

The historical values of solar radiation arriving at the top of the Earth's atmosphere and on the Earth's surface were determined from data on luminosity relative to the present time from the time at which the sun entered the main sequence of stars, 0.031×10^9 y after formation, to 6.5×10^9 y in the future (Sackmann et al., 1993). The available solar energy received at the top of the atmosphere and absorbed at the Earth's surface were determined from the luminosity data as well as data on the temperature of the sun (Sackmann et al., 1993), assuming that the temperature of the CBR remained unchanged at 2.725 K. The surface temperature on the Earth has not been constant over geologic time and this condition may also be true for some arbitrary height in the Earth's atmosphere, which means that the background condition for calculating solar exergy received by the Earth may change over time for any environment other than the CBR. These data were applied to calculate b^* (Petela, 1964) from which the kJ of exergy m^{-2} s^{-1} arriving at the top of the atmosphere were determined. The present factor of 30% attenuation by the atmosphere was assumed to hold across time to give an estimate of the solar exergy absorbed on the surface of the Earth.

Table 2
Definition and values for the symbols identifying forcing functions and flows in Fig. 2. System components are identified but not evaluated. Most values in this table are calculated from the average value of the Earth energy budgets reported in Table 7 Column 5 gives a reference to the place in this paper or in another paper, where the calculation of the values reported in column 3 can be found. In this table, the energy generated by the eroded mass of the continents falling through a distance is assumed to be equal to the heat dissipated in uplifting an equal mass to balance erosion.

Item	Symbol	Value	Units	Reference
Emergy inflows				
Solar emergy received, top of atmosphere	EmS_R	$55{,}063 \times 10^{20}$	seJ y^{-1}	Table 5
Solar emergy absorbed, Earth's surface	EmS_A	$38{,}544 \times 10^{20}$	seJ y^{-1}	Table 5
Solar emergy absorbed in the atmosphere	$EmAtm_A$	$16{,}519 \times 10^{20}$	seJ y^{-1}	By difference
Forcing functions				
Inflow to land (solar emergy)[a]	J_1	$11{,}563 \times 10^{20}$	J y^{-1}	Table 5
Chemical potential of rain on land[b]	J_2	5.10×10^{20}	J y^{-1}	Campbell (2003)
Inflow of gravitational energy[c]	J_3	1.17×10^{20}	J y^{-1}	Table A2
Temperature				
Average temperature of the mantle	T_M	2339	K	Sorokhtin et al. (2011)
Average temperature of the ocean bottom	T_{OC}	275.2	K	Sorokhtin et al. (2011)
Carnot Ratio (efficiency)	$(T_M - T_{OC})/T_M$	0.882		This table
Components				
Mass continental crust	CC		g	NA
Mass oceanic crust	OC		g	NA
Mass mantle	M		g	NA
Mass core	C		g	NA
Radioactive material in the continental crust	R_{CC}		g	NA
Radioactive material in the oceanic crust	R_{OC}		g	NA
Radioactive material in the mantle	R_M		g	NA
Radioactive material in the core	R_C		g	NA
Heat stored in the continental crust	H_{CC}		J	NA
Heat stored in the oceanic crust	H_{OC}		J	NA
Heat stored in the mantle	H_M		J	NA
Heat stored in the core	H_C		J	NA
Gravity-chemical potential energy in mantle	GC_M			
Flows on pathways				
Exergy of eroded mass of the continents[d]	J_4	8.86×10^{16}	J y^{-1}	Table A3
Exergy of isostatic uplift of continents	J_5	?	J y^{-1}	NA
Exergy of mass uplifted by plate motion[ed]	J_6	?	J y^{-1}	NA
Exergy of uplift of $J_5 + J_6$[e]		8.86×10^{16}	J y^{-1}	Table A3
Exergy of ocean plates sinking	J_7	?	J y^{-1}	NA
Exergy of new oceanic crustal growth	J_8	?	J y^{-1}	NA
Exergy flow in tectonic processes, $J_6 + J_7 + J_8$[f]		9.20×10^{20}	J y^{-1}	Table 7, note b
Exergy of mass sinking from mantle to core[g]	J_9	?	J y^{-1}	NA
Exergy of mass rising from core to mantle[g]	J_{10}	?	J y^{-1}	NA
Heat dissipated by the tides[h]	h_1	1.17×10^{20}	J y^{-1}	Table A2
Solar heat dissipated in erosion of land[i]	h_2	11552×10^{20}	J y^{-1}	$J_1 + J_2$
Heat flow required for isostatic uplift of land[j]	h_3	1.63×10^{20}	J y^{-1}	Table 7, note b
Heat flow driving ocean plate movement[k]	h_4	7.57×10^{20}	J y^{-1}	Table 7, note b

[a] Solar transformity at the Earth's surface is set as 1 sej J^{-1} = seJ J^{-1}; therefore, the global inflow of solar radiation absorbed at the Earth's surface is assumed to be the inflow of solar emergy supporting the system. The solar radiation that falls on the continents (30% of surface area) contributes to erosion through heating and cooling of the Earth's surface.

[b] The chemical potential energy of rain on land is used, in part, in chemical weathering of the land and geopotential energy of water is used in erosion; therefore, the global solar emergy is required for erosion.

[c] The gravitational energy of the Moon and Sun is absorbed by the Earth's mass as body forces acting within the core, mantle and crust and as work done on the ocean bottom through tidal dissipation. In the former case the energy dissipated is small and distributed throughout the Earth, thus on average it makes no substantial contribution to the heat gradient. In the latter case the heat of tidal energy dissipation on the ocean bottom opposes the heat gradient driving plate motion.

[d] The exergy of the eroded mass of the continents is relative to sea level. The value used is from the Pleistocene (Table A3), which is the latest data point for which the erosion estimate was not affected by agriculture.

[e] The exergy of uplift is calculated relative to sea level. The components of uplift are difficult to evaluate separately but over millions of years a reasonable assumption is that the exergy of uplift and erosion are in balance (Table A3).

[f] The components of the Earth Cycle are difficult to evaluate separately, but the exergy flow driving tectonic processes is required for the operation of the entire cycle (Table 7, note b).

[g] The exchange of exergy flows between the core and mantle was not evaluated.

[h] All of the energy of gravitational attraction entering the Earth is assumed to be dissipated.

[i] The heat energy dissipated in erosion of the land mass through heating and cooling and chemical weathering of the surface.

[j] The deep heat flow from the Earth required for isostatic uplift through the concentration of lighter lithospheric materials at the surface is assumed to be the heat flow through the continents and shelves minus the heat generated in CC (Fig. 2) by radioactive decay (Table 7). This is equal to the part of the Earth's heat flow supporting uplift.

[k] The part of the Earth heat flow driving tectonics, plate motion and the consequent uplift of the continents that occurs as a result (Table 7, note b). The sum of h_3 and h_4 is the Earth exergy dissipated to support the Earth cycle.

3.3.2. *Method of estimating tidal geopotential energy over time*

This calculation was possible because Kagan (1997) compiled estimates of variation in the major lunar semidiurnal component of the tides, M_2, over the past 10^9 y with values for the early Cambrian given for a period centered on 555,000,000 y BP. Kagan (1997) drew on several different studies to obtain the data and different methods were used to make the estimates. The reader is referred to the original studies for more detailed information (Table A1). The tidal exergy dissipated in the world oceans was estimated by using the information in Munk and Wunsch (1998) to expand the estimates of M_2 given in Kagan (1997) and by adjusting Kagan's estimate using the measurements of M_2 made by Egbert and Ray

(2000). These estimates were possible because of the assumption that the relationships between the M_2 tidal component and the other lunar components, and between the M_2 component and the Earth tide, have been relatively constant over the time of the estimates, i.e., the past 2.5×10^9 y. Also, the relationship between solar exergy and the geopotential exergy it generates was assumed to have been constant over the time within a given generation regime, i.e., ice-covered or ice-free polar oceans.

3.3.3. Method of estimating the Earth cycle over time

This calculation was possible because Wilkinson and McElroy (2006) estimated the volume of sediment deposited in the world oceans from the Cambrian to the present time (i.e., over the past 542,000,000 y). The exergy of the mass of sediments eroded from the continents was calculated using the formula, $U = gmh$, where g is gravity, m is the mass of sediments eroded and h is the average height of the landmass. An average density for the continental land mass of 2.8 g cm^{-1} (Condie, 1993) was used as were historical values for the average elevation of the continents from Sorokhtin et al. (2011). Most of the additional data needed to make estimates of the exergy flows over the past 555,000,000 years (Table A3) were found in Sorokhtin et al. (2011). Since some of the values needed were unknown or uncertain earlier than 555,000,000 y BP; this analysis focused on constructing the emergy baseline of the Earth over the last 555,000,000 y. Also, of necessity the calculation was performed for the average value over long periods of time for which the erosion regimes were established, thus while annual flows are evaluated they do not translate to any particular year, but instead to a time increment in the history of the Earth over the last 5.55×10^8 y (Table A3).

3.4. Method for checking the transformity of the exergy of the ocean tides

Our estimates for the transformities of the exergy of tidal geopotential energy or deep Earth heat can be checked, if another independent process can be found that depends on two or more of the three quasi-independent sources of available energy to the Earth. Riguzzi et al. (2009) found that the vertical movements caused by the Earth tides are too small to drive plate motion (0.25% of the tectonic exergy flow) based on data in Ray et al. (1996) and Sorokhtin et al. (2011). However, they point out that the horizontal, permanent torque caused by the misalignment of the tidal bulge on the surface of the Earth and the gravitational trajectory of the Earth–Moon system provide an amount of kinetic energy loss (~2.3 TW, Knopoff and Leeds, 1972) that could result in motion of the lithosphere. Earlier work on this subject by Bostrom (1971) first presented arguments for the westward displacement of the lithosphere caused by the fact that the oceanic and solid Earth tidal bulges lead the overhead position of the Moon, so that the sum of the resulting coupled forces is between 3.9 and 5.3×10^{23} dyne cm^{-1} calculated from the acceleration of the moon in its orbit and the reduction in the Earth's rotation rate (Munk and Macdonald, 1960). Bostrom (1971) argued that this force was sufficient to displace the lithosphere westward around the mantle lying below it. The rate of displacement is dependent on the resultant forces and the viscosity of a thin layer in the upper mantle upon which the shell of the Earth would rotate. Observation of variations in the velocity of seismic waves indicate that such a low viscosity layer exists (Knopoff, 1972), but there is still some uncertainly about the depth of the layer and the actual value of its viscosity (Doglioni et al., 2014). These factors are crucial in determining the amount of rotation of the lithosphere that can be expected from the applied forces. Bostrom (1971) cites several pieces of evidence that imply that the lithosphere is rotating westward. For example, he states, "Westward drift will not be apparent to us; but it will appear that surface features related to the underlying mantle, for example persistent volcanic rock sources, have a tendency to migrate east." In a recent paper, Doglioni et al. (2014) state that "... all plates, albeit at different velocity, move westerly along a curved trajectory with a tectonic equator tilted about 30° relative to the geographic equator." In other words, the position of the hot spot on the Earth's surface remains practically unchanged, since its origin is below the low viscosity zone in the stationary mantle, but it appears to have moved, because of the westward translation of the lithosphere. Further arguments supporting the westward displacement of the lithosphere as a function of gravitational forces of the Earth and Moon are given in the references mentioned above. This evidence appears to be strong enough to use the westward displacement of the lithosphere as the basis for a calculation to check our estimate of the solar equivalence of the energy of gravitational attraction.

In this method, the motion of the plates driven by the underlying convection cells in the mantle is assumed to be a separate mechanism from the westward plate motion generated by the tidal couple on the Earth's lithosphere. Thus, it is plausible that these two processes are acting in superposition to create the movements of the Earth's lithosphere and the two motions can be considered independently in a first order calculation. In both cases the mass and motion of the Earth's crust generated by each process can be estimated and given that frictional effects at the boundary layer are similar; the kinetic energy required to move the lithosphere a given distance in a year over the underlying mantle can be calculated. The kinetic energy dissipated in moving the lithosphere is assumed to be the same regardless of the process causing the movement. Under this assumption, the tidal exergy equivalence of the kinetic energy dissipated in the annual westward movement of the lithosphere and the Earth exergy equivalence of the kinetic energy of plate motion can be calculated and then related to one another to give the Earth heat transformity of the tidal exergy. The solar exergy equivalence of the exergy of deep Earth heat is known and using that a second estimate for the solar transformity of the tides can be made.

The formula for kinetic energy, K.E. = $1/2mv^2$, where m is the mass moved and v is the velocity, was used to determine the energy of crustal motion. The mass moved was determined from the crustal volume of the oceanic basins and marginal seas in the first case and of the oceanic crust and the continental crust after continental crustal volume was corrected for the volume of shields and platforms in the second case. Shields and platforms have deep roots that are "sticky" areas in the movement of the lithosphere (Bostrom, 1971; Knopoff, 1972). Data on the average thickness and density of the crust at different locations were used to determine the mass moved. The average velocity of plate movement was determined by doubling the average half-spreading rate for all plates given in Conrad and Lithgow-Bertelloni (2007). Velocities for the westward displacement of the lithosphere were calculated using the estimate of Bostrom (1971) and for a conservative range of values (Doglioni et al., 2014), who also supplied a maximum value assuming the presence of an unverified, thin, very low viscosity layer at the mantle-crust boundary. The detailed calculation method and supporting notes used to check the estimate of the solar exergy equivalence of tidal exergy dissipated are given in Table 3.

4. Results

4.1. Solar radiation

Solar radiation supplies the largest amount of energy and available energy to the Earth, e.g., the solar energy absorbed by the Earth at the surface is about 2686 times larger than the second largest

Table 3
An alternative method for estimating the solar equivalence of tidal exergy based on the westward displacement of the lithosphere and plate movement driven by tectonic processes.

Parameters	Plate movement[a]	Lithosphere or shell rotation[b]			
		0.2°/10^6 y	0.4°/10^6 y	0.46°/10^6 y	1.0°/10^6 y
Mass[c], m (g)	7.96×10^{24}	1.57×10^{25}	1.57×10^{25}	1.57×10^{25}	1.57×10^{25}
Plate Velocity, v (cm s^{-1})	1.57×10^{-7}	7.06×10^{-8}	1.41×10^{-7}	1.62×10^{-7}	3.53×10^{-7}
Kinetic Energy[d], K.E. (J s^{-1})	9.83×10^{3}	3.90×10^{3}	1.56×10^{4}	2.06×10^{4}	9.75×10^{4}
Available energy[e], Earth, E (J y^{-1})	9.20×10^{20}	NA	NA	NA	NA
Available energy[f], tide, T (J y^{-1})	NA	1.17×10^{20}	1.17×10^{20}	1.17×10^{20}	1.17×10^{20}
Earth Equivalence K.E.[g], T_E (J J^{-1})	2.97×10^{9}	NA	NA	NA	NA
Tidal equivalence K.E.[h], T_G (J J^{-1})	NA	9.49×10^{8}	2.37×10^{8}	1.79×10^{8}	3.80×10^{7}
Ratio equivalences[i], T_E/T_G	NA	3.14	12.56	16.61	78.48
Solar equiv. Earth Cyc.[j], T_{EC} (seJ J^{-1})	4200	NA	NA	NA	NA
Solar equivalence tide[k], τ_G (seJ J^{-1})	NA	13184	52737	69745	329609

[a] Plate movement is two times the global average value of the half spreading rate given by Conrad and Lithgow-Bertelloni (2007).
[b] The rates of net rotation of the lithosphere with respect to the mantle are given in Doglioni et al. (2014) with 0.2° to 0.4°/10^6 y bracketing the conservative range of estimates measured with respect to the rate of movement of the crust relative to the position of hotspots in the Pacific and a faster rate of 1.0°/10^6 y that might be possible, if a very low viscosity layer exists at the crust-mantle boundary. The 0.46°/10^6 y is equivalent to the value put forward by Bostrom (1971), when he first estimated the westward displacement of the lithosphere.
[c] The mass of the moving plates was calculated from the area of the oceans and marginal basins, 3.086×10^8 km^2, (Sclater et al., 1980), the average thickness of the oceanic plates, 8.6 km (Mooney et al., 1998) and average oceanic crust density of 3.0 g cm^{-1}, i.e., the maximum estimate in Carlson and Raskin (1984). The mass of the lithosphere shell under rotation was calculated as the sum of the mass of the oceanic plates plus the fraction (1–0.69) times the mass of the continents or the mass of the continental crust after shields and platforms have been subtracted (Christensen and Mooney, 1995). Area data were taken from Sclater et al. (1980) as follows: continents, 1.49×10^8 km^2, continental shelves, 5.22×10^7 km^2. An average thickness of 38 km was assumed for the continents (Mooney et al., 1998) and a thickness of 19 km was estimated for the continental shelves using the following logic: Fox et al. (1970) estimated that the continental shelf off Hispaniola was 2× the thickness of the oceanic crust (e.g., 17.2 km) and Mooney et al. (1998) give a minimum for continental crust thickness of 20.5 km (for extended crust), which result in an average shelf crust thickness estimate of about 19 km. The density of the continental crust was assumed to be 2.8 g cm^{-1} from Condie (1993).
[d] Kinetic energies of plate movement and shell rotation are compared assuming that the frictional effects at the low viscosity boundary layer are similar. Multiply by seconds per year to calculate annual ratios.
[e] The available energy or exergy of the Earth heat flow driving plate movement is given in Table 2.
[f] The available energy of the gravitational attraction of the Moon and Sun (i.e., tides) is given in Munk and Wunsch (1998). In this case, the entire tidal energy input to the Earth (3.7 TW) drives the westward displacement of the lithosphere.
[g] The Earth exergy equivalence of the kinetic energy of plate movement is the annual Earth exergy inflow divided by the kinetic energy of plate motion.
[h] The tidal exergy equivalence of the kinetic energy of the rotating lithosphere is the annual tidal exergy inflow divided by the kinetic energy of lithospheric rotation.
[i] The ratio of the Earth exergy equivalence of plate movement to the tidal exergy of lithosphere rotation shows the relative efficacy of these two sources of available energy in moving the Earth's crust.
[j] The solar exergy equivalence of the Earth Cycle was determined as the rounded average from estimates in Table 8 and Table A4.
[k] The solar exergy equivalence of the tide can now be estimated by multiplying the relative efficacy of the tides in moving the lithosphere compared to the Earth Cycle by the solar exergy equivalence of the Earth Cycle.

energy source, i.e., the heat energy exiting through the Earth's surface. In this section, the solar energy and solar exergy arriving at the top of the Earth's atmosphere and absorbed on the Earth's surface are calculated for the present time, followed by a calculation of the solar exergy received and absorbed by the Earth from its origin to 5×10^9 y into the future, a time period over which the output of the sun is expected to be fairly stable (Sackmann et al., 1993).

4.1.1. Present value of the solar energy and solar exergy input to the Earth

Estimates of the solar energy received by the Earth at the top of the atmosphere and absorbed at the surface of the Earth are given in Table 4. In this paper, the energy received is distinguished from the energy absorbed by the system, as recommended in Campbell et al. (2005).

Estimates of the available solar energy or solar exergy received at the top of the Earth's atmosphere and absorbed at the surface of the Earth are given in Table 5. Solar exergy was calculated relative to the temperature of the CBR at the edge of the atmosphere and to the average temperature of the surface of the Earth using the method in Petela (1964).

4.1.2. Time history of solar radiation arriving on Earth

The historical values of solar radiation arriving at the top of the Earth's atmosphere and on the Earth's surface are given in Fig. 3. There has been a steady increase in the emissive power of the Sun from the time it entered the Main Star Sequence, shortly after its formation, to the present time (i.e., 4.6×10^9 y from the origin).

4.2. Gravitational attraction of the Moon and Sun

The gravitational attraction of the Moon and Sun is the third largest input of available energy to the Earth. The solar energy absorbed on the Earth's surface is 33,000 times greater than the gravitational energy supplied by the Moon and Sun. In this section, the components and interactions of the gravitational attraction of the Moon and Sun on the Earth are used to calculate equivalence between solar exergy and the exergy of the ocean tides using the

Table 4
Incident solar radiation: solar energy arriving on the Earth from the Sun.

The Solar Constant[a]	Cross Sectional Area[b]	Top of the Atmosphere[c]	On the Earth's Surface[d]
1366 W m^{-2}	1.278×10^{14} m^{-2}	5.509×10^{24} J y^{-1}	3.856×10^{24} J y^{-1}

[a] An average value for the solar constant was determined from data in Fig. 1 of Foukal et al. (2006) by averaging the averages (white lines in Foukal's Fig. 1) for periods of high and low total solar irradiance (W m^{-2}) as measured by radiometers on various spacecraft from 1978 to 2006.
[b] Radius of the Earth is 6.3871×10^6 m at the Equator (Weast, 1981).
[c] Multiply the solar constant by the cross sectional area of the Earth and the number of seconds in a year.
[d] Assume that on average losses in the atmosphere from scattering and absorption equal 30% of that incident at the top of the atmosphere (ITACA, 2011).

Table 5
Incident solar radiation: available solar energy (exergy) arriving on the Earth from the Sun at the top of the atmosphere (received) and on the Earth's surface (absorbed). Exergy calculations are based on the equations in Petela (1964). Exergy is relative to the Earth's average surface temperature in Row 1 and to the temperature at the top of the atmosphere in Row 2.

Temperature[a] sun (K)	Temperature[b] background (K)	b* Solar emissivity[c] ($kJ\,m^{-2}\,s^{-1}$)	Solar exergy received[d] ($W\,m^{-2}$)	Top of atmosphere ($J\,y^{-1}$)	Earth's surface ($J\,y^{-1}$)
5781	287.15	59,093.64	1276.5	5.1449×10^{24}	3.6014×10^{24}
5781	2.725	63,251.24	1366.2	5.5063×10^{24}	3.8544×10^{24}

[a] The temperature of the sun can be estimated using the Stephan–Boltzmann Law and the radius of the sun = 695,508 km (NASA, 2014a) and was found to be 5800 K (http://ircamera.as.arizona.edu/astr_250/Lectures/Lecture_12.htm). The observed solar constant at the top of the atmosphere and the relationships for the sun's emissivity and the exergy of radiation arriving on Earth in Petela (1964) were used to back calculate the sun's temperature in Table 5, which is close to 5800 K.
[b] The exergy of solar radiation arriving on the Earth was calculated relative to the average global temperature from 1951 to 1980 of 287.15 K (NASA, 2014b) and to the temperature of the cosmic background radiation (CBR) outside of the Earth's atmosphere, 2.725 K (NASA, 2014c).
[c] Eq. (5) in Petela (1964) was evaluated using the solar and background temperatures given in this table.
[d] Petela's evaluation of Eq. (42) and calculations of b^* were used together to estimate the exergy received in the solar radiation arriving on Earth when the background temperature is considered to be just outside the top of the atmosphere and when it is considered to be at the surface of the Earth.

evaluated model in Fig. 1. Finally, the results of model output and data analysis given in Kagan (1997) are used to reconstruct a time history of tidal energy dissipation in the world oceans over the past 2.5×10^9 y.

4.2.1. Exergy inflow due to the gravitational attraction of the Moon and Sun

The exergy of gravitational attraction of the Moon and Sun is transmitted to the Earth in several forms and at several frequencies. The largest quantity of this available energy is dissipated by the tides in the world oceans (3.5 TW), with a much smaller quantity dissipated in the solid Earth tides (0.2 TW) and even less in the tides of the atmosphere (0.02 TW). The value of the M_2 component alone is 2.5 TW. These values and a detailed evaluation of the tidal energy inputs to the Earth can be found in Munk and Wunsch (1998).

4.2.2. The solar transformity of the ocean tides

The equivalence between solar exergy and the exergy of the ocean tides was determined by evaluating ESL models for two quasi-stable states of the Earth's geobiosphere (Fig. 1A and B). Fig. 1A shows The Earth with polar ice, as it is today and as it has been to a greater or lesser degree (Zachos et al., 2001) for approximately the last 34×10^6 y or since Antarctica became glaciated (Deconto and Pollard, 2003). When the polar oceans are ice-covered there is a smaller total water surface area that can become stratified; and therefore; the geopotential energy generated annually by solar exergy is less ($1.089 \times 10^{20}\,J\,y^{-1}$) compared to the solar geopotential energy of $1.596 \times 10^{20}\,J\,y^{-1}$ generated over the greater ocean surface area of an Earth with ice-free polar oceans (Oort et al., 1994). The variable efficiency with which solar exergy creates geopotential energy in the world oceans leads to a solar exergy equivalence of 24,200 seJ J^{-1} for the available energy dissipated by ocean tides, when the oceans are ice-free compared to a solar equivalence of 35,400 seJ J^{-1} for tidal exergy when the polar oceans are ice-covered (see the equations evaluated on Fig. 1B and A, respectively). The data, sources, and assumptions used in these calculations are given in Table 6.

4.2.3. Time history of the tidal exergy dissipated in the world oceans

Estimates of the available energy dissipated by ocean tides over the past 2.5×10^9 y are given in Appendix A, Table A1 and in Fig. 4. These estimates are based on Kagan (1997), who synthesized the results of 4 studies of Earth–Moon tidal evolution of the M_2 tidal component over the past 1×10^9 y and model results (Kagan and Maslova, 1994) for the period from 1.0×10^9 to 2.5×10^9 y BP. The

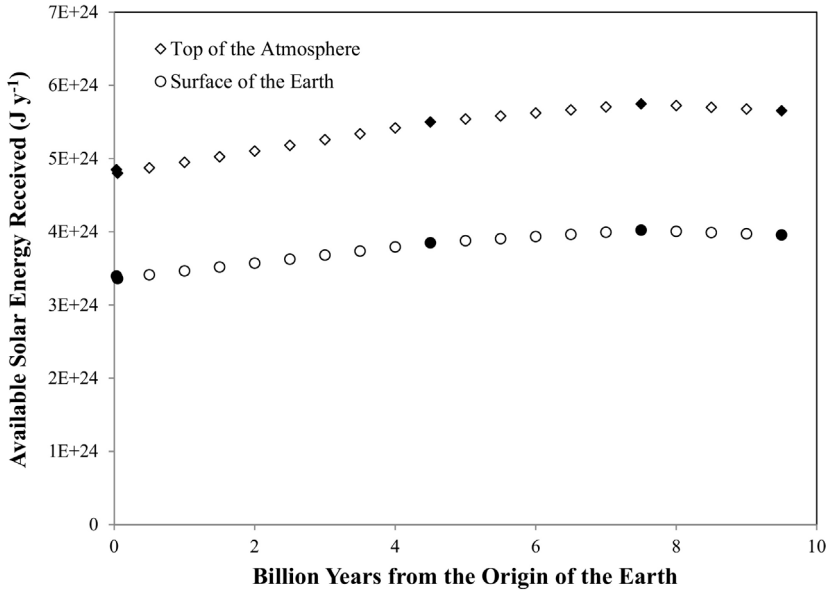

Fig. 3. Available solar energy received at the top of the atmosphere and on the surface of the Earth, assuming the attenuating properties of the atmosphere have not changed over time. The time shown covers the stable period of the sun's life history, i.e., from the time it entered the main sequence of stars to around 10 billion years after its formation (Sackmann et al., 1993). Solid data points are calculated from data on the Sun's age, luminosity and temperature (Sackmann et al., 1993) by applying the formulae used earlier (Petela, 1964) to estimate the solar exergy received by the Earth based on the Sun's emissivity.

Table 6
Calculation of the equivalence between solar and tidal exergy based on the geopotential energy dissipated in the world oceans from the available energy supplied by the Sun and the gravitational attraction of the Moon and Sun. Following Oort et al. (1994), $D(P)$ is the potential energy generated, $D(K)$ is the kinetic energy dissipated and $D(S)$ is the total energy dissipated in the oceans from solar sources. $D(T)$ is the tidal energy dissipated in the oceans and $D(S+T)$ is the total geopotential energy dissipated. All values are in joules per year ($J\,y^{-1}$). Solar emergy is equivalent to solar exergy by assumption. See Appendix A, Table A2 for detailed calculations.

	$D(P)$	$D(K)$	$D(S)$	$D(T)$	$D(S+T)$	$\%S$	$\%T$	T_{tide}
Polar Ice[a]	4.44×10^{19}	6.44×10^{19}	1.09×10^{20}	1.10×10^{20}	2.19×10^{20}	0.496	0.504	35,393
Without polar ice[b]			1.60×10^{20}	1.10×10^{20}	2.70×10^{20}	0.591	0.409	24,165

[a] Data on $D(P)$, $D(K)$ and $D(S)$ from Oort et al. (1994). Data on $D(T)$ from Munk and Wunsch (1998).
[b] Data on $D(S)$ from Oort et al. (1989) with turnover time of 1.36 years calculated from Oort et al. (1994) applied to the potential energy estimate of Oort et al. (1989). Data on $D(T)$ from Munk and Wunsch (1998).

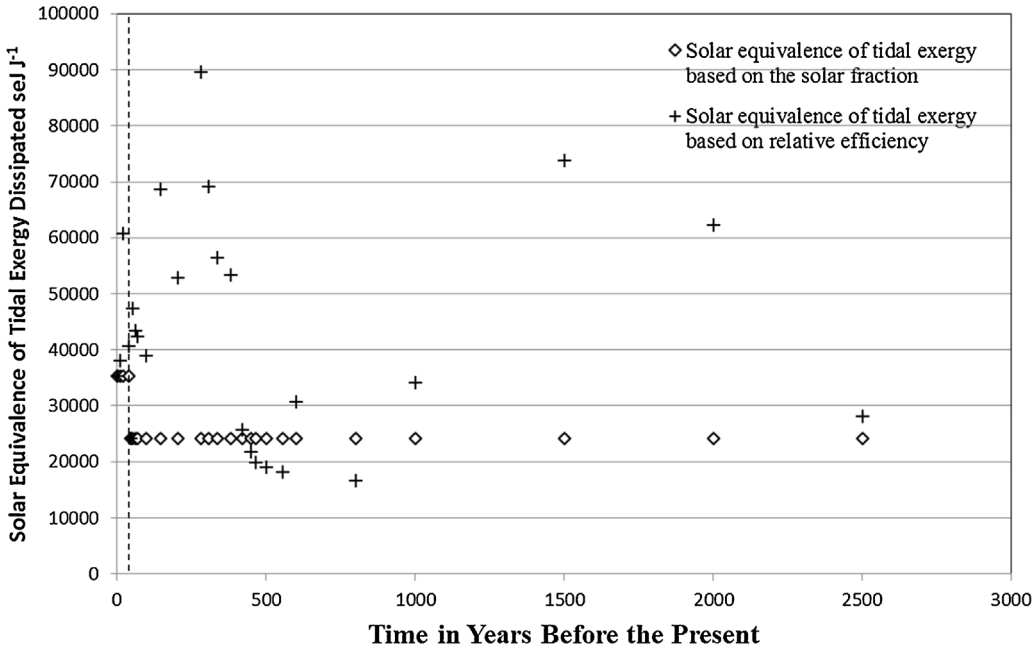

Fig. 4. Variation of the solar equivalence of ocean tidal exergy over the past 2.5×10^9 y with 0 being the present. Diamonds show the solar equivalence of tidal exergy dissipated in the oceans for two configurations of the Earth's surface, ice-covered and ice-free polar oceans. Here the solar-derived geopotential energy of the oceans determines the equivalence between solar and tidal exergy. The solid diamonds represent conditions for the present and for 3.8×10^7 y BP, which are the base years for the two configurations of the Earth's surface. The dashed line shows the boundary between the recent regime of ice-covered polar oceans and the prior period when the polar oceanic area was ice-free. The crosses show what the equivalences between solar and tidal exergy would have been based on the amount of tidal exergy dissipated globally compared to that dissipated in the base year for the two periods (black diamonds).

estimates based on the M_2 tidal component were "scaled-up" as explained in the notes to Table A1 using the information in Munk and Wunsch (1998) to estimate the total tidal exergy dissipated in the world oceans over this time.

4.2.4. Time history of the transformity of the tides in the world oceans

Estimates of the time history of the solar equivalence of the ocean tides over the past 2.5×10^9 y are given in Appendix A, Table A2. The time series estimates and the data needed to calculate them are shown for two modes of the Earth System, i.e., with polar ice, after 38×10^6 y BP and without polar ice, earlier than 38×10^6 y BP with the transition point at 38×10^6 y BP determined by the resolution of the estimates given in (Kagan, 1997). The solar equivalence of the tidal energy dissipated in the world oceans is shown over the past 2.5×10^9 y (Fig. 4) along with the estimated solar equivalence of the tidal exergy dissipated, if the equivalences are adjusted based on the relative efficiency of the Earth as a "machine" for generating tidal geopotential energy (Table A2). For example, tidal resonance is greater when the continental land masses are distributed over the surface of the Earth and less when the land masses come together as supercontinents. A plot of changes in the relative efficiency of the Earth in generating tidal exergy (Fig. 5) shows that the present tidal exergy dissipation in the oceans is

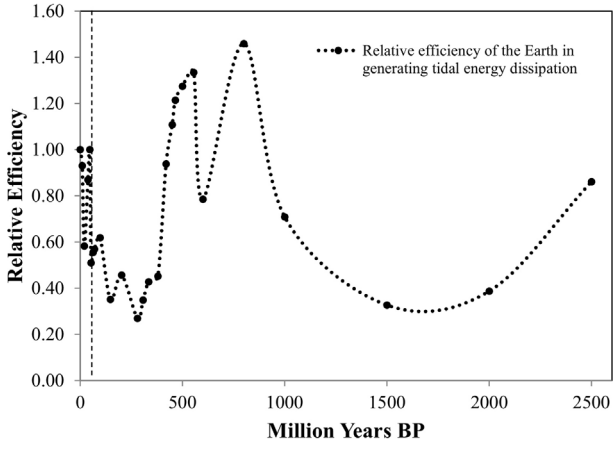

Fig. 5. Variation of the relative efficiency of tidal exergy generation in the world oceans from the present to 2.5×10^9 y BP due to changes in the position of the land masses on the surface of the Earth. The plotted values are determined by the tidal resonances set-up as the positions of the continents changed with time. The dashed line separates the present world with ice-covered polar oceans from the world without ice-covered polar oceans. Efficiencies are expressed relative to the latest value in these two time periods. Values are only estimated for the points plotted and the dotted line is added for convenience to make it easier to follow changes in the solar transformities of the tides through time.

Table 7
Current heat budgets for the solid Earth. Energy flows are in terawatts (TW).

Source	Oceans + seas	Continental radioactivity	Continents + shelves	Global total	Total with hot spots[a]	Earth cycle[b]
Heat flows including hydrothermal circulation						
Mareschal et al. (2012)	29	7.6 ± 1.9	14	43	46	31.2
Davies and Davies (2010)	31.9		14.7	45.7	46.7	34.8
Sorokhtin et al. (2011)	33.9	9.1		43		33.9
Jaupart et al. (2007)	32	7	14	43	46	34.8
Pollack et al. (1993)	31.2		13.1	44.2		32.4
Sclater et al. (1980)	30.4		11.5 ± 2.1	42		31.2
Heat flow: Average ± SD	31.4 ± 1.7		13.5 ± 1.2	43.5 ± 1.3		33.0 ± 1.7
Heat flows without hydrothermal circulation						
Hofmeister and Criss (2005)	19.4		11.6	31.0		19.2
Davies and Davies (2010)	21.3		14.7	36.0	37	24.2

[a] Hot spot heat flow is the difference between the "Global Total" and "Total with Hot Spots". Estimates range from 1 to 3 TW. Because of their nature as single point outflows of heat, hot spots were not included in the heat flows driving the Earth Cycle of uplift and isostatic adjustment.
[b] Heat flow driving the Earth Cycle is estimated as the heat flow through the oceans and seas minus the heat gained by the oceanic lithosphere (2.9 TW, Sclater et al., 1980) minus the heat generated by radioactive decay in the oceanic crust (1.3 TW, Sclater et al., 1980); plus the average heat flow through the continents and shelves, minus the average heat flow from radioactive decay in the continental crust (Mareschal et al., 2012). The Carnot Ratio (0.8818) was then applied to obtain the exergy numbers for h_3 (isostatic) and h_4 (tectonic) processes in Fig. 2.

at the highest point seen over the past 38×10^6 y, which is about 171% higher than its value in the Early Miocene around 20×10^6 y BP (Table A1).

4.3. Heat flow through the surface of the Earth

Recent studies of heat flow through the surface of the Earth are summarized in Table 7. The heat flow through the oceans and seas is separated from the heat flow through the continents and continental shelves. Also, the heat generated by radioactive decay in the continental and oceanic crust is reported separately. The heat flow estimates are reported in two categories: (1) heat flow including model estimates of the heat removed through the ocean crust by hydrothermal circulation and (2) the Earth heat flows actually measured that do not incorporate model estimates of hydrothermal flow. The estimates of the heat flow driving the tectonic processes of the Earth and contributing to isostatic adjustment of continental elevations are listed under "Earth Cycle" in Table 7. Sorokhtin et al. (2011) provide a direct estimate of this flow. The other estimates in this column were calculated from the information given in this table using the method described in note b. The average value of the heat flow driving tectonic processes of the Earth was 33.0 ± 1.7 TW based on the six global heat flow budgets that included the heat flux due to hydrothermal circulation. If the hypothesized heat flow lost through hydrothermal circulation is not included, the heat flux driving the Earth Cycle is about 10 TW less than if it is present.

4.3.1. Evaluated model of the Earth cycle driven by solar and deep Earth heat exergy

An evaluated ESL model of the Earth at the present time was used to determine the equivalence between solar exergy inflow and the exergy of deep heat flow from the Earth (Fig. 2). The values, units and references for all forcing functions and flows shown in Fig. 2 are given in Table 2. In this model the available energy dissipated by erosion of land mass from the surface of the continents (0.00089×10^{20} J y^{-1}) is assumed to be balanced by the available energy of total uplift (i.e., from isostatic adjustment and plate movements) over long time periods, e.g., 10 million years or longer. The total exergy of the heat flow dissipated in driving the Earth Cycle was 9.20×10^{20} J y^{-1} (Fig. 2, $h_3 + h_4$) and the solar exergy driving the process was 3.85×10^{24} seJ y^{-1}.

4.3.2. The solar equivalence of the exergy of deep Earth heat flow

A value of 4191 seJ J^{-1} for the solar transformity of deep Earth heat used to drive tectonic processes is estimated in Fig. 2 and Table 8. The solar transformity of Earth heat flow is determined from the geopotential energy dissipated, relative to sea level, by the erosion of the mass of the continents due to the actions of sun and rain, under the assumption that the upward mass flux of land from isostatic adjustment and tectonic uplift, again relative to sea level, balances the mass removed by erosive processes over the long run, e.g., ten million years. Thus, the available energy dissipated in erosion is assumed to be equal to the available energy dissipated in land uplift.

Table 8
Calculation of the solar exergy equivalence of the Earth heat exergy driving the Earth Cycle.

Solar exergy[a] (J y^{-1}), (seJ y^{-1})	Earth cycle[b] energy (J y^{-1})	Earth heat exergy[c] (J y^{-1})	Exergy erosion[d] (J y^{-1})	Solar equivalence erosion[e] (sej J^{-1})	Earth exergy equivalence land uplift[f] (seJ J^{-1})	Solar equivalence Earth heat[g] (seJ J^{-1})
3.854×10^{24}	1.043×10^{21}	9.202×10^{20}	8.859×10^{16}	4.350×10^{7}	1.038×10^{4}	4191

[a] Solar exergy received at the surface of the Earth, i.e., the solar exergy absorbed by the Earth.
[b] Earth Cycle heat energy flux is the average of the values for the heat flow supporting the Earth Cycle including hydrothermal circulation from Table 7.
[c] The available energy in the Earth heat flow is the heat flow in column 2 multiplied by the Carnot ratio (0.882) calculated for the difference between the average temperature of the mantle, 2339 K (Sorokhtin et al., 2011, p. 190) and the average temperature at the bottom of the oceans, 275.15 K (Sorokhtin et al., 2011, p. 500).
[d] The exergy of erosion is calculated in Appendix A, Table A3.
[e] The planetary solar exergy absorbed is divided by the potential energy dissipated in erosion of the continental land mass to obtain the solar equivalence of the exergy dissipated in erosion.
[f] The exergy of the Earth heat flow supporting tectonic processes is divided by the exergy dissipated in the uplift of a land mass equal to that eroded to obtain the Earth heat equivalence of the available energy dissipated in uplift.
[g] The ratio of the solar equivalence of the potential energy dissipated through erosion to the Earth heat equivalence of the available energy dissipated in uplift is the solar transformity of the Earth exergy flow supporting the Earth Cycle.

4.3.3. Historical time series of erosion and deep Earth heat flow

The history of erosion of the continental land mass of the Earth, since the Cambrian period 5.42×10^8 y BP is given in Table A3. This reconstruction was made using data on erosion reported by Wilkinson and McElroy (2006) and estimates of average continental elevations from Sorokhtin et al. (2011). Data on the area of the continents, the volume of sediment deposited, the erosion rate, the erosion mass flux, the average height of the continents and the exergy of the mass eroded from 5.42×10^8 y BP to the present are given in Table A3. The exergy dissipated by the eroded mass falling through a distance was calculated relative to sea level assuming that the average density of the continents is 2.8 g cm^{-1} (Condie, 1993) and the acceleration due to gravity is 9.81 m s^{-2}.

4.3.4. Historical time series of the solar equivalence of deep Earth heat exergy flow

The data and calculations needed to determine the values of the solar equivalence of the exergy of the deep Earth heat flow is given in Table A4. The estimates of the exergy of erosion were transferred from Table A3 and combined with data from Sorokhtin et al. (2011) on Earth Cycle heat flow, the average temperature of the mantle and the average sea floor temperature from 5.55×10^8 y BP to the present (Table A4). The Carnot ratio, calculated from the temperature gradient between the average mantle temperature and the temperature at the sea bottom, varied from 0.8720 to 0.8817, a 1.1% increase over the time examined. In contrast, the solar equivalence of the exergy of deep Earth heat varied from 3064 to 4258 seJ J^{-1} or a 39% increase over 5.55×10^8 y. The time series of data and the consequent estimates of transformities in Table A4 are based primarily on the data in Sorokhtin et al. (2011); therefore, they are somewhat different from the average values for the same quantities calculated from the average of six Earth heat budgets given in Table 7.

4.4. Summary of the exergy inflows to the Earth

The exergy inflows to the Earth system from the Sun, the Earth's deep heat driving tectonic processes, and the exergy dissipated by ocean tides are shown in Fig. 6 over the entire period for which data were available for each input. The solar exergy input to the Earth has increased gradually at a steady rate over the entire time since 0.031×10^9 y after the formation of the Earth (Sackmann et al., 1993). The exergy dissipated by the Earth in tectonic activities has a distinct peak about 2.6×10^9 y BP corresponding to the approximate time of core formation (Sorokhtin et al. (2011). From about 2.2×10^9 y BP to the present, the amount of exergy dissipated in driving the Earth Cycle has steadily declined. The exergy dissipated through oceanic tides is plotted over the past 2.5×10^9 y. The variability of the tidal exergy dissipated in the world oceans has been presented earlier, but here again it is apparent that it has been quite variable over the past 1×10^9 y compared to the other exergy inflows to the Earth.

4.5. The present emergy baseline for the Earth

The planetary baseline for the Earth at the present time, i.e., for a world with ice-covered polar oceans, is calculated in Table 9

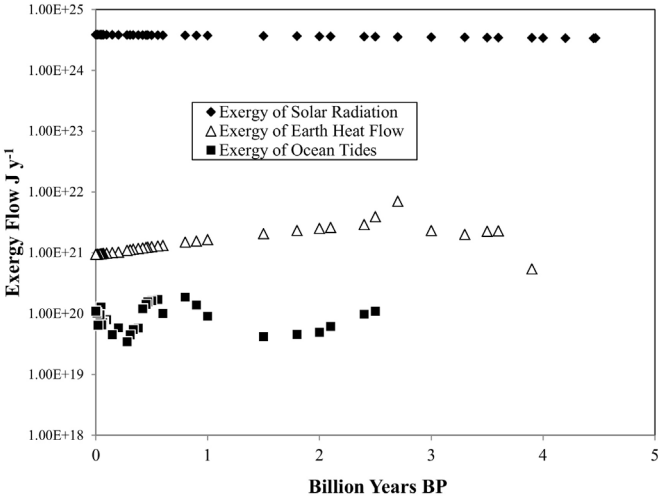

Fig. 6. Exergy inflows to the Earth as solar radiation, the deep Earth heat driving the Earth Cycle and the tidal geopotential exergy dissipated in the world oceans, each is shown over the longest period for which an estimate could be made with 0 being the present time.

based on the determinations of the solar exergy equivalences of the oceanic geopotential exergy dissipated (35,393 seJ J^{-1}) and for the exergy dissipated in the heat flow supporting tectonic processes (4191 seJ J^{-1}). The baseline determination resolves to a value of 1.16×10^{25} seJ y^{-1} with a split of approximately 1/3, 1/3, and 1/3 in the implied organizing power of the three independent inflows based on the emergy that they deliver to the Earth.

Also, the emergy baseline of the Earth was determined for conditions when the polar oceans are ice-free (Table 10). In this case the average transformities for the exergy of the oceanic geopotential dissipated (24,100 seJ J^{-1}) and for the exergy dissipated in supporting the Earth Cycle (3607 seJ J^{-1}) were used in the calculation of the baseline over the period from 555,000,000 to 38,000,000 years BP. In this case the baseline determination resolved to a value of 9.828×10^{24} seJ y^{-1} with a split in the implied organizing power in the proportion of 1:0.58:1, Sun:Tide:Earth.

4.6. The planetary baseline of the Earth over the past 555,000,000 years

Calculations of the emergy baseline of the Earth and the emergy input of the Sun, Earth and Tides over the past 555,000,000 y are presented in Table A5 and plotted in Fig. 7. Using the data from Sorokhtin et al. (2011) for the Earth heat flow and including both the tidal states with and without polar ice-covered oceans; the average emergy baseline for the Earth over the past 555,000,000 y was $1.00 \times 10^{25} \pm 1.13 \times 10^{24}$ seJ y^{-1} (Table A5). The value of the baseline at the present time using the historical time series data is 1.16×10^{25} seJ y^{-1} (Fig. 7). The variability of the planetary baseline is largely determined by the variation of the emergy supplied by the ocean tides (Fig. 7), since the emergies supplied by the Sun and Earth exergy flows have been fairly constant over this time. The planetary baseline traces a U shaped pattern over the past 5.55×10^8 y, primarily due to the period from 3.8 to 1.5×10^8 y BP

Table 9
Planetary baseline for the present time, i.e., for a world with polar ice, using the average estimate for heat flow and average solar equivalences for Earth's deep heat exergy flow and ocean tidal exergy dissipation.

Energy source	Exergy inflow (J y^{-1})	Equivalence (seJ J^{-1})	Solar Eq. inflow (seJ y^{-1})	Fraction
Solar radiation	3.854×10^{24}	1	3.854×10^{24}	0.332
Ocean tidal dissipation	1.105×10^{20}	35,393	3.911×10^{24}	0.337
Earth's tectonic heat	9.202×10^{20}	4191	3.857×10^{24}	0.332
Total solar equivalent inflow			1.162×10^{25}	1.001

Table 10
Planetary Baseline from 555,000,000 to 38,000,000 years BP, i.e., a world without polar ice, calculated using the average exergy inflows and transformities for the three sources of available energy over this time.

Energy source	Exergy inflow (J y^{-1})	Solar Equiv. (seJ J^{-1})	Solar Eq. inflow (seJ y^{-1})	Fraction
Solar radiation[a]	3.791×10^{24}	1	3.791×10^{24}	0.386
Ocean tidal dissipation[b]	9.167×10^{19}	24,100	2.210×10^{24}	0.225
Earth Cycle heat[c]	1.061×10^{21}	3607	3.827×10^{24}	0.389
Total solar equivalent inflow			9.828×10^{24}	1.000

[a] The solar radiation received by the Earth has been increasing over time.
[b] Data from Kagan (1997).
[c] Data from Sorokhtin et al. (2011). The Earth Cycle's heat flow was decreased over time either from depletion of iron in the mantle in the cold body model or from core and secular cooling in the hot body model of Earth's origin.

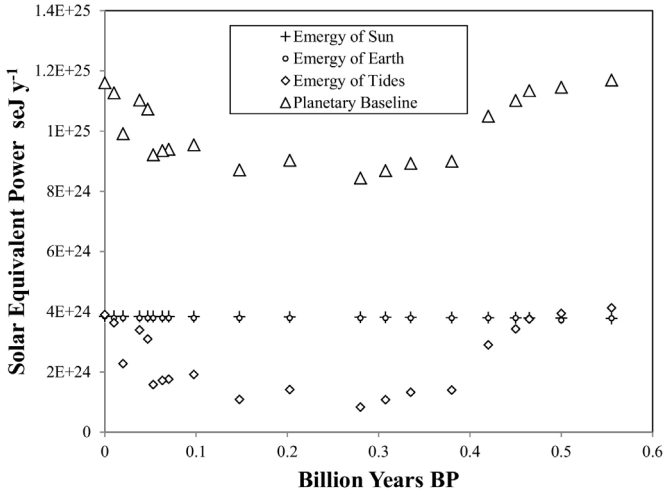

Fig. 7. The emergy baseline for the planet and the contributions of emergy received from its component parts, the Sun, S; the Earth, E; and the Tides, G from the present time to 555,000,000 y BP.

when the Earth's land masses were joined together as the supercontinent, Pangaea, and planetary tidal exergy generation was lower.

4.7. An alternative method to calculate the solar equivalent exergy of the ocean tides

Calculations of the solar equivalent exergy of the tidal exergy dissipated in the oceans based on equating the kinetic energy dissipated annually by the available energy of the Earth's deep heat flow moving the continental plates with the kinetic energy dissipated annually by the available energy of the tidal forces driving the westward rotation of the Earth's lithosphere are given in Table 3. The midpoint ($0.3^{\circ}/10^{6}$ y) of the most plausible range of rotation for the westward displacement of the lithosphere (Doglioni et al., 2014) gives an estimate of 32,961 seJ J^{-1} for the solar equivalent exergy of the exergy of tidal energy dissipation compared to the value of 35,393 seJ J^{-1} estimated in Table 6. Remarkably, there is only a 7.3% difference between these two estimates.

5. Discussion

One of the weaknesses in the present body of emergy studies is the lack of methodological consistency caused by the fact that several planetary baselines are in common use. The goal of this paper is to provide the community of scientists with a more accurate estimate for the planetary baseline of the Earth for use as a basis for the determination of transformities in emergy evaluations and in environmental accounting (Odum, 1996). In Section 4, the baseline for the Earth's geobiosphere was calculated for the present and over the past 555,000,000 y by establishing solar equivalences for the Earth's deep heat exergy flow and for the tidal exergy dissipated in the world oceans. Extensive documentation was given so that these values and the method for obtaining them will be transparent and easy to understand. This was done with the hope that the new baseline will be recognized as being based on sound science and that it is better documented and more plausible than past estimates; and therefore, it might be readily adopted in the future by scientists doing emergy studies.

In this section, the importance of the planetary baseline for emergy evaluations is discussed followed by a brief summary of the reasons that a new study is needed at this time. Next the question, "Is the emergy baseline really arbitrary?" is considered. The new models used to calculate equivalences are compared to past models and the way that past conceptual and empirical errors were corrected or avoided in the new models and calculations is summarized. Next, the uncertainty and variability in the models and data used in this paper and the magnitude of possible errors introduced by such uncertainties is estimated, in so far as this is possible. The plausibility of the method used to check our calculations of the solar equivalence of tidal exergy is examined. Finally, the implications that the new calculation methods for determining the solar equivalence of Earth's deep heat flow have for calculating the emergy supplied to surface processes from within the Earth are examined.

5.1. The efficacy of emergy as a comprehensive accounting mechanism

The maximum empower principle (Lotka, 1922a,b; Odum, 1996) indicates that, over sufficiently long periods of time, the forces of evolutionary competition will ensure that all available energy flows will develop feedbacks within the system that have effects on increasing energy flow in the system commensurate with their production costs, i.e., in proportion to their minimum transformities or their transformities at maximum empower (Odum, 1996; Campbell, 2001; Tilley, 2015). Thus, in a hierarchical system that has had time to adapt to its inputs, as is the case for the Earth over its 4.6×10^{9} year history, smaller, rarer, available energy inflows, e.g., the Earth's deep heat and the tides would be expected to develop more powerful amplifying effects per unit feedback within the system. For example, research in plate tectonics during the 1960s and 1970s made it apparent that the Earth would be a dead planet, if not for the relatively small flows of available energy from within the Earth driving plate movements (Sorokhtin et al., 2011). The beauty and power of emergy accounting is that a single quality-adjusted quantity (i.e., emergy measured as solar emjoules) can be used to quantify all processes, products, and services derived within the Earth's geobiosphere on an equal basis by reference to a planetary baseline for which the equivalences between the different exergy inflows to the system have been established. In this way, all kinds of energy, material and information gain or loss in the system can be accounted for in equal terms as solar emergy.

Thus far, no other accounting scheme has been able to achieve such a unified and comprehensive approach to quantifying the value of system components and flows. Emergy evaluation and environmental accounting in its present form would not be possible without establishing a planetary baseline that expresses the disparate energy inputs from the sun, deep Earth heat and gravitational attraction on a common basis first as solar equivalent joules (seJ) by establishing the equivalences among the exergy inflows as described above. Once the planetary baseline has been established as solar equivalent exergy all quantities generated by Earth processes can be quantified as solar emergy, sej, i.e., by applying the track summing method beginning from the baseline, now unified as one inflow of solar equivalent joules, where one seJ in the baseline is equal to 1 solar emjoules, sej of the emergy base supporting the development of all subsequent planetary processes.

5.2. The need for a new calculation of the planetary baseline

In Section 2.2, the reasons for recalculating the planetary baseline at this time were presented in detail. These reasons range from the development and maturation of a new theory of the evolution of the Earth (Sorokhtin et al., 2011) through geophysical misunderstandings in the formulation of models used to determine both the equivalence between solar radiation and deep Earth heat flow, and solar radiation and the geopotential energy of the world oceans to a simple misreading of Earth's heat budget as reported in Sclater et al. (1980). However, the misinterpretations derived from this misreading led to major errors in the formulation and evaluation of the energy sources contributing to "crustal heat". Therefore, a new calculation of the planetary baseline was carried out in this study.

5.3. Is the emergy baseline of the Earth arbitrary?

It is a common notion in scientific and engineering studies that reference lines are arbitrary, when the results of analyses are expressed relative to the reference line; and therefore, the import of such results does not change, if the reference line changes. The same is true of the results of emergy evaluations, when converted from one baseline to another, if only the relative changes between states or alternatives are to be considered. However, the value of the emergy baseline will affect the outcome of an emergy evaluation, when adjustments are made to the baseline to avoid undercounting (see Section 2.2.1). The scientific assumption that baselines can be arbitrary is a powerful simplification that allows research and analysis to answer questions in a relativistic manner without being encumbered by the often difficult task of establishing the absolute value of variables. However, there are often bio-physical boundaries in a natural system where one set of boundaries or conditions is more plausible as a baseline for analysis that other choices, e.g., sea level and the elevation divides that establish watersheds. Also, the choice to use emergy methods can imply that the investigator is bringing into play a deeper level of understanding about the boundaries and baselines that may be appropriate for a system that is grounded in thermodynamics. At this deeper level of characterization, the choice of a planetary baseline is not entirely arbitrary, and alternatives can be discriminated as better or worse based on their conformation, or lack thereof, to observations and to the principles of Energy Systems Theory (Odum, 1994, 1996).

Specifically, the operation of the maximum power principle (Lotka, 1922a,b) leads to testable corollaries, such as the predictions that (1) the power of an input to organize its system is expected to be proportional to the emergy delivered to the system by that input and (2) the emergy delivered by inputs with lower transformities will be matched by inputs with higher transformities, to make products of intermediate transformity, so that the emergy delivered by both sources will be maximized over time. Predictive principles, such as these can be useful in discriminating between alternative baselines from the standpoint of their consistency with the Energy Systems Theory (Table 1). For example, when the fraction of solar equivalent energy input from each of the quasi-independent energy sources to the Earth was calculated for the present time, the fraction of the solar equivalent energy delivered by the inputs was revealed to be approximately 1/3, 1/3, 1/3, which is consistent with the prediction of Energy Systems Theory that an optimum matching of high (tidal exergy), intermediate (Earth deep heat exergy) and low (solar exergy) quality inputs will develop over time in the Earth's geobiosphere. As a result, the empower contributed to the system by each of the interacting quasi-independent inputs is maximized (Table 9). This is an important result that strongly suggests that the emergy baseline of the Earth is not arbitrary, because the Earth system appears to have evolved toward the matching of inputs to attain maximum power over time.

5.4. Evaluated models used to determine the solar equivalence of tidal geopotential energy

The formulation of the models used to determine the equivalences between solar radiation and the geopotential energy dissipated annually by the tides differ from those used in most past studies. First, estimates are presented for two states of the Earth system, with and without ice-covered polar oceans, which differ in their potential to generate geopotential energy from the solar exergy received (Oort et al., 1994). Calculation of the solar transformity of the tides is based on the available energy dissipated in the oceans, rather than on the available energy generated, and thus it includes the annual flow of both potential and kinetic energy (Oort et al., 1994). In this study, it was recognized that the numbers in Oort et al. (1989, 1994) should be applied to the solar portion of the geopotential energy only and thus the tidal geopotential energy dissipated in the oceans (3.5 TW) was added to the geopotential generated by solar processes to get the total in Table 6. Sufficient information was given in these two papers to allow us to calculate a turnover time for the annual geopotential energy generated in the world oceans (1.36 y), which was assumed to be 1 year in Campbell (2000a) and Odum (2000). The total geopotential exergy dissipated in the world oceans for a world without ice-covered polar oceans (2.70×10^{20} J y^{-1}) includes the amount dissipated annually derived from solar energy (1.60×10^{20} J y^{-1}) plus the amount dissipated annually by the ocean tides (1.10×10^{20} J y^{-1}).

In all evaluations, the pull of the gravitational forces of the Moon and Sun create geopotential energy in the oceans; however, the role of Earth heat flow in creating oceanic geopotential energy is treated differently in our model compared to the models of Odum (2000) and Brown and Ulgiati (2010). The method used in the current paper for establishing equivalence between solar radiation and the oceanic geopotential energy dissipated by the tides was to quantify the solar-based processes generating geopotential energy in the oceans on the scale of one year. The long term effects of the Earth Cycle on tidal geopotential energy dissipated are handled separately using a model that depicts this change as a modification of the relative efficiency of the position of the land masses on the surface of the Earth as "a machine" for generating tidal geopotential energy. In contrast, Odum (2000) and Brown and Ulgiati (2010) used a highly aggregated model of the Earth system to make estimates of the solar transformity of the annual generation of the exergy of the tides by assuming that the Earth's deep heat flow contributes to the annual creation of geopotential energy in the world oceans on an equal basis with the annual solar and tidal exergy generation processes. This model, as shown earlier (Section 2.2.3), is only valid over very long time scales.

5.5. Evaluated models of the generation of oceanic geopotential energy over long time periods

The long term variability of tidal exergy generation in the world oceans was modeled explicitly as shown in the ESL models in Fig. 1A and B. In contrast, the available energy flows driving this variability are subsumed within the determination of the present equivalences between solar radiation and tidal geopotential energy in the models used by Odum (2000) and Brown and Ulgiati (2010). The data in Kagan (1997) indicate that the efficiency of this "machine" for generating tidal exergy varies over long time periods with the changing position of the continents on the surface of the Earth, because the tidal geopotential energy generated in the oceans is largely dependent on the resonant frequencies set up by the tidal harmonics interacting with the basin sizes that are created by the changing position of the continents (Kagan, 1997). This interaction is indicated in Fig. 1 by the variable coefficient, k_v, which is located within a box indicating the process generating tidal geopotential energy. This coefficient represents the variable efficacy of the configuration of the continents in generating tidal geopotential energy and the resulting variability in tidal exergy dissipation in the world oceans over long time periods. In a plot of the time history of the relative efficiency of the tidal exergy generation process (Fig. 5), the magnitude of this variability ranges from 0.27 times the base ice-free value at 2.8×10^8 y BP to 1.46 times this value at 8.0×10^8 y BP. The average coastal system in the world would look very different under this degree (5.4 fold) of variability in tidal exergy generation as can be inferred from examining the emergy signatures of and physical conditions in Cobscook Bay, ME, a macro-tidal system, and Mosquito Lagoon, FL, a system with low tidal exergy inputs (Campbell, 2000b).

In this study, the slow movement of the continental plates over the surface of the Earth is recognized to have resulted in two quasi-stable states of the Earth's surface that are responsible for generating different quantities of solar geopotential energy in the world oceans (Oort et al., 1994). As a result, the presence or absence of polar ice-covered oceans results in two different solar transformity regimes for the generation of tidal exergy in the oceans. The coefficients k_1 and k_2 (Fig. 1A and B) located within the small boxes indicating the process of geopotential energy generation by solar processes, respectively; represent the state of the world with land masses distributed around polar oceans and the state of the world with the continental land masses distributed so that there are no ice-covered polar oceans. The time series estimates of the solar transformity of the ocean tides (Fig. 4) and the data needed to calculate them are shown for these two modes of the Earth System (Fig. 1).

Due to the resolution of the data, 38×10^6 y BP was plotted as the transition point between a world with and without polar ice. However, the actual transition point is somewhere between the initiation of the growth of ice sheets in Antarctica at 34×10^6 y BP (Deconto and Pollard, 2003) and 8.0×10^6 BP, the time when Zachos et al. (2001) indicate that the transition to a world with heavily ice-covered polar oceans was complete. As a result, the current state of the Earth's surface and the planetary baseline derived from it may be somewhat younger than indicated by the transition point between ice-free and ice-covered polar oceans used in the figures.

The historical variability of the tidal exergy generated in the world oceans indicates that the transformity of the geopotential energy created from solar sources sets the larger system context for the generation and dissipation of tidal exergy. Therefore, the base transformity for the two ocean regimes mentioned above is determined by the solar transformity of the geopotential energy dissipated from solar sources. The amount of tidal exergy dissipated in the oceans at any particular time will be a function of the efficacy of the configuration of the continents in producing tidal resonance; thereby, generating more or less tidal exergy in the world oceans over time. Such variations will account for a greater or lesser role of tidal exergy in the planetary baseline and in its power to organize the geobiosphere, subject to the solar geopotential energy regime currently in operation.

5.6. Evaluated models used to establish the solar equivalence of the Earth's deep heat flow

Both Odum (2000) and Brown and Ulgiati (2010) combined their models for evaluating the solar equivalence of crustal heat flow with their model for determining the solar equivalence of the tidal geopotential energy to generate a system of two equations and two unknowns, which they solved for the solar equivalences of the two inputs. Putting aside the problems related to the errors in Odum and Odum (1983)'s evaluation of the Earth's heat budget (Section 2.2.2.2), these models represent depictions of the Earth system that are only valid over very long time periods, yet they are applied to analyze the annual generation of exergy flows. In contrast, the model shown in Fig. 2 evaluates a particular process, i.e., the Earth Cycle, on the basis of one year, which at this scale is driven by erosion of the continents and by deep heat flowing from the mantle to the surface, driving convection in the mantle and the tectonic processes of the Earth, i.e., uplift from plate movements and isostatic processes.

Fig. 2 shows that the heat generated by gravitational attraction on the solid Earth is distributed throughout the body; therefore, it cannot make a positive contribution to the deep heat gradient of the Earth. Furthermore, the heat dissipated by tidal friction on the bottom of the ocean cannot increase the heat gradient driving Earth processes, since it warms the low temperature endpoint i.e., the ocean bottom. This is different from the models used by Odum (2000) and Brown and Ulgiati (2010), who did not evaluate a particular process to determine the equivalence between deep Earth heat and solar radiation. Instead they determined the transformity of a constructed geophysical quantity that they called "crustal heat". In Odum (2000), this heat flow is largely composed of the heat flow from mantle convection, which was missed in translating the heat budget of Sclater et al. (1980). In the model in this paper, the heat from radioactive decay generated in the Earth's crust does not contribute to the heat gradient driving tectonic processes (Sclater et al., 1980; Sorokhtin et al., 2011). However, it is a contributor to crustal heat in the models of Odum (2000) and Brown and Ulgiati (2010). A problem arises with the concept of "crustal heat", because the decay of radioactive elements in the lithosphere is a "dead" geologic process[14], i.e., this heat flow makes little, if any, contribution to the dynamic tectonic processes of the Earth (Sorokhtin et al., 2011). To calculate the solar equivalence of the exergy of deep heat flow driving tectonic processes, i.e., plate and isostatic uplift, the exergy dissipated in eroding mass from the surface of the continents was assumed to be equivalent to the exergy dissipated in the uplift of an equal mass of rock from below sea level to some average height above sea level. The ratio of the solar equivalent exergy of the exergy dissipated by the eroded mass to the Earth heat exergy of the exergy of the uplifted mass is then equal to the solar exergy equivalence of deep Earth heat. This concept is relatively easy to understand and it results in a plausible relationship between the relative contributions of the exergy of solar radiation, deep Earth heat, and tidal energy in the planetary baseline.

[14] The decay of radioactive elements in the crust is considered to be ineffectual in terms of driving tectonic process, because they have been separated by density-chemical differentiation into the less dense lithosphere, and thus removed from contributing to the heat gradient driving the tectonic processes of the Earth (Sorokhtin et al., 2011).

5.7. Evaluated models of the solar equivalence of Earth heat flow over long time periods

The geologic processes operating the Earth Cycle were evaluated over the past 555,000,000 y as described in Tables A3 and A4 using data on erosion from Wilkinson and McElroy (2006) and data on other ancillary parameters from Sorokhtin et al. (2011). Erosion is measured in three ways by Wilkinson and McElroy (2006): (1) over long periods of time from the lower Cambrian up to the Pliocene, it was measured by the volume of sedimentary rock deposited in the different geologic time periods, (2) in recent times, i.e., starting in the Pleistocene, it was measured by the transport of sediment by large rivers and (3) in the present the estimate included runoff from agricultural lands. In order to establish a modern baseline prior to major anthropic alterations of the cycles of the elements (Campbell et al., 2014), an estimate of erosion based on the flow of large rivers was used to represent erosion in the present time (value in red and underlined in Table A4). In the future, it may be worthwhile to look at the influence of humanity on the mass flux of sediments, comparing erosion including agriculture with erosion based on the transport of sediments by large rivers alone.

5.8. Energy, exergy and emergy basis for the geobiosphere

The exergy basis for the geobiosphere indicates that the Sun is 3 orders of magnitude greater than the exergy of Earth heat flow and 4 orders of magnitude greater than the exergy inflow from the gravitational attraction of the Moon and Sun. If exergy was indicative of the organizing power operating the geobiosphere, the work done would be almost entirely explained by the input of solar exergy as was assumed by Chen et al. (2010) in their cosmic exergy accounting method and there would be little need to consider the work of the Earth heat flows and the tides within the system. Emergy gives a different picture of the processes driving the organization of the Earth (Fig. 7). Once the inputs have been adjusted for the quality of the exergy, solar radiation and deep heat flow from the Earth are shown to have contributed approximately equal organizing power to the geobiosphere over the past 5.55×10^8 y; whereas, the organizing power contributed by tidal exergy has ranged from 22% of the solar emergy inflow in the Early Permian, 2.80×10^8 y BP, to 109% of the solar input in the Early Cambrian, 5.55×10^8 y BP. The present generation of tidal emergy in the geobiosphere is in the upper portion of its range over the past 5.55×10^8 y and the average tidal emergy inflow over the entire time period is only 64% of the currently inflowing solar exergy. Therefore, at the present time, the coastal regions of the world are comparatively rich in emergy inflow and the organizing power delivered to these ecosystems is high.

In review, the similarity between the equivalences established between solar exergy and the exergy of the deep Earth heat flow and tidal geopotential to simple ratios of the energy inflows of solar energy to Earth heat energy and tidal energy was brought forward. These relationships are now examined in Appendix B, Table B1. While there is no immediate causal connection between the energy inflows of the sun, Earth deep heat, and tide, these flows are the underlying basis for the exergy calculations applied in this study, so perhaps it is not surprising that there are some similarities in the two sets of ratios. However, these ratios are also quite different, especially with regard to the transformity of the Earth's deep heat flow, which was 49.2% greater than might be expected from a simple ratio of the energy flows. Similarly, the transformity of the tide for ice-free polar oceans, which was 26.7% greater than might be expected based on the energy ratio of solar to tidal energy (Table B1). The calculations in this paper are carefully supported with logical arguments and data, whereas there is no apparent justification for thinking that simple ratios of the energy inflows would give reasonable approximations to the equivalences sought. Nevertheless, these energy ratios are in the general "vicinity" of the exergy ratios calculated here. Even though it is the exergy flows that are determining the equivalences in this paper, a working hypothesis is that the relationships of solar energy to the other two energy inflows will also move toward values consistent with condition in which each of the different quality inputs are contributing approximately equal organizing power, i.e., emergy.

5.9. The choice of an emergy baseline for carrying out emergy evaluations and its future

The pattern of the emergy baseline over the past 5.55×10^8 y has been driven by the variation in the tidal emergy generated (Fig. 7), which in turn has been determined by the configurations of the continents created by their slowly changing positions. For the practical purpose of carrying out emergy evaluations in a uniform manner, a value for the emergy baseline must be chosen. The present value of the baseline is 1.16×10^{25} seJ y^{-1} and its average value over the past 5.55×10^8 y is 1.00×10^{25} seJ $y^{-1} \pm 1.13 \times 10^{24}$ seJ y^{-1}. While it is tempting to recommend the value 1.00×10^{25} seJ y^{-1} because of its simplicity, emergy evaluations and transformities should probably be referenced to the current value of the baseline, which is 1.16×10^{25} seJ y^{-1} in this study. Adjustments off of this baseline can be made using the 1/3, 1/3, 1/3 distribution of organizing power among the inflows. As mentioned earlier, this distribution of organizing power among the emergy inflows to the Earth can be predicted from the principle of emergy matching to achieve maximum empower in a network of flows.

EST posits that the geobiosphere or any other system must be exposed to a given spectrum of emergy inflows for a sufficient period of time to adapt its structure and function to the system's prevailing emergy signature (Campbell, 2000b). Rapid or sudden changes in the relationships of the inflows may result in perturbations to the system during the time necessary for adaption to the new signature. The current decrease in polar ice over the Arctic ocean (Comiso, 2002) that appears to be driven by increasing temperatures at high latitude (Rothrock and Zhang, 2005) that, in turn, may be a consequence of increased atmospheric CO_2, represents a change in the geobiosphere that may result in a potentially significant change to the planetary baseline. If the decrease in Arctic sea ice continues over the next 100 years as predicted in Comiso (2002), the planetary emergy baseline and the organizing power of the tides may move temporarily toward the values for a world with ice-free polar oceans (Table 10). However, if the present polar ice melts, the geobiosphere will need time to adjust its network of flows to maximize empower in the new state. Nonetheless, the ice-free state is probably transient, because the supplies of fossil fuel that are the source of excess CO_2 in the atmosphere are finite. In addition, Sorokhtin et al. (2011) predict that the long term trend of the Earth is toward a colder climate and the continuation of polar ice-covered oceans.

5.10. Uncertainty in the models and data used

This study relied on a particular, self-consistent treatise on the evolution of the Earth (Sorokhtin et al., 2011) to provide the background information that along with other data has allowed us to carry out the historical portion of this study. Sorokhtin et al. (2011) is predicated on the assumption that the primordial Earth was a cold body with homogenously distributed matter. Conventional wisdom in Europe and America follows the assumption that the Earth began as a hot body. This distinction is important for the early history of the Earth, but it makes little difference for our study of the emergy baseline over the past 5.55×10^8 y, because by this time the heat flow from the Earth under both models has stabilized and is in

a smooth near linear decline (Fig. 6). For example, Fig. 6 in Labrosse and Jaupert (2007) gives a present oceanic heat flow of 34 TW from a model of the average secular cooling rate of the Earth, which gives an estimate of the transformity of deep Earth heat of 4222 seJ J^{-1}, which is practically identical to the estimate obtained from data derived from a cold core origin.

In general, much of the scientific knowledge about the interior of the Earth has been gained by inference and this condition has generated and continues to generate controversy. In this study, plausible estimates for all of the parameters used were documented, but in all cases other data and opinions might have been chosen instead. This uncertainty in the body of geophysical research is acknowledged; therefore, in the future geophysicists may develop a better understanding of the processes upon which this evaluation of the planetary baseline of the Earth is based.

5.10.1. Uncertainty in the data used to calculate the solar transformity of the tides

The values for the available energy of the tides are fairly accurate, since they are based on astronomical considerations (Sorokhtin et al., 2011); however, the most accurate values are the estimates of the M_2 tidal component, which is the largest component of tidal exergy. The value of the M_2 component (2.5 TW) has recently has been verified empirically (2.436 ± 0.009 TW) through laser altimetry (Egbert and Ray, 2000). This measured value is within 2.6% of the theoretically determined value. In general, a reduction in uncertainty of the estimates of tidal exergy has resulted from more complete measures of the tidal exergy inflows. Similarly, improvements in the estimates of oceanic geopotential energy have been associated with incorporating more complete data on the inputs or through obtaining a better understanding of the nature of the physical system under study.

For example, in Odum (2000) the amount of tidal energy input to the oceanic geopotential energy (2.7 TW) is only that dissipated in shallow water by the lunar semidiurnal components (Miller, 1966), whereas Brown and Ulgiati (2010) used the total tidal energy received by the oceans and the solid Earth (3.7 TW) from Munk and Wunsch (1998). The data from Munk and Wunsch (1998) is more complete, since it includes the oceanic lunar semidiurnal components, the other lunar components, as well as the solar diurnal components along with the tides in the solid Earth. This more complete estimate of the tidal input is 37% larger than the original inputs considered in Odum (1996). The tidal energy input to models in Fig. 1 (3.5 TW) is 29.6% larger than the input used by Odum (1996), thus the uncertainty of the estimate is reduced by incorporating the more complete measures of the tidal energy inflows. Of course, this assumes that the model including the more complete flows is correct in the first place.

Odum (2000), Campbell (2000a,b) and Brown and Ulgiati (2010) used 2.14×10^{20} J y^{-1} from Oort et al. (1989) as an estimate of the total oceanic geopotential energy created annually. In this study, the uncertainty of this number was reduced by incorporating insights from Oort et al. (1994), who pointed out the number in Oort et al. (1989) actually refers to conditions in a world with ice-free polar oceans. Reformulating the relationship resulted in a measure of the total geopotential energy for a world without ice-covered polar oceans that is 26% larger than the original number. However, when the ice-covered polar oceans today are considered the reformulation results in a corrected number for the total geopotential energy of the oceans that is only 2.3% larger than the number used in the papers listed above. In this case a reduction in model uncertainty did not lead to a large change in the value of the estimate, but the overall calculation becomes considerably more certain because a valid model of the physical process was used.

5.10.2. Uncertainty in the heat budget of the Earth

The principal uncertainty in measuring the heat flow through the surface of the Earth involves the question of the existence and magnitude of hydrothermal heat flows through the ocean bottom. The problem arises from the fact that there is a discrepancy between the heat flow measured at the seafloor and the higher values of heat flow predicted by models of the cooling lithosphere (Stein and Stein, 1994). Hydrothermal flows through the crust that remove heat are hypothesized to be the explanation of this discrepancy. Specifically, the heat flux measured near mid-ocean ridges is considerably less than one would predict from the magmatic heat sources present there (Elderfield and Schultz, 1996). Objections to the attribution of large heat flows to hydrothermal circulation focus on the models used to predict these heat flows (Parsons and Sclater, 1977; Stein and Stein, 1994). Hofmeister and Criss (2005) criticize these models based on their use of a constant coefficient to estimate heat flux; whereas, they argue that this coefficient is a function of temperature; and therefore, decreases with depth leading to heat flows smaller than predicted. They also argue that large hydrothermal flows away from the Mid-Ocean Ridge axis are not expected.

However, there is physical evidence supporting the existence and magnitude of hydrothermal flows from observations and measurements made on the ocean bottom (Corliss et al., 1979; Mottl and Wheat, 1994). Measurements taken around the Galapagos rift indicated that 2/3 of the heat lost from new oceanic lithosphere may be lost through thermal springs (Corliss et al., 1979). Another study of this area (Williams et al., 1974) using a sampling grid of 71 stations found that about 80% of the heat released near the ridge crest came from hydrothermal flows. Most authors (Table 7) accept the characterization of the Earth's heat budget that includes hydrothermal flows of about 9 TW (Elderfield and Schultz, 1996). However, Davies and Davies (2010) also provide an estimate of 36 TW for Earth heat flow without considering hydrothermal circulation. If hydrothermal circulation was removed from three of the heat budgets shown in Table 7, the solar exergy equivalence of deep Earth heat would be 5650 seJ J^{-1} or 35% greater than our average estimate of 4200 seJ J^{-1}, which includes the heat flow from hydrothermal circulation. Both the conventional wisdom of geophysicists and the body of evidence to date indicate that hydrothermal flows contribute to the heat flux through the surface of the Earth; therefore, this perspective was used in determining the planetary baseline of the Earth. Variability in the measurements of the heat flow driving tectonic processes was shown to be ±5% for 6 heat budgets that included hydrothermal flows.

5.10.3. Reduction in data and model uncertainty as a result of the new baseline calculation

By discovering and correcting the errors incorporated in the baseline estimates of Odum and Odum (1983), Odum (1996) and Campbell (2000a) and by comparing these earlier estimates to the current analysis, estimates of the reduction of uncertainty in the baseline calculation related to the data and models used can be made. Comparing Odum (1996) to Campbell (2000a,b) and recognizing that the model used in Campbell (2000a) to calculate the tidal energy input is a methodological improvement over Odum (1996), the uncertainty in the baseline estimate was reduced by 1.9% (9.44–9.26)/9.26). If the corrected heat budget and the corrected value for the geopotential of the world oceans are mainly responsible for the difference between the current estimate of the baseline and that made by Odum (1996) and Campbell (2000a), correcting the data accounted for a reduction of 17.2% and 18.8%, respectively, in the uncertainty of the baseline estimates. Finally, if the baseline estimates of Odum (2000) and Brown and Ulgiati (2010) differ from the current estimate, because of differences in

both the models and data used to determine the baseline, the current estimate results in decreasing the uncertainty of the estimate of the baseline by 38.9% and 33.3%, respectively. These reductions in uncertainty depend on the likelihood that the data used in this study is more accurate than that used in earlier studies and that the model used in this study is more plausible than earlier models.

5.11. Implications of the present study for the emergy evaluation of Earth processes

The Earth Cycle is the fundamental geologic process that makes the Earth a "living" planet, i.e., a planet with an active surface crust, unlike the Moon, which is not presently a tectonic body. Other Earth processes, e.g., volcanism, earthquakes, may have different transformities and will have to be evaluated in the future.

In addition, the method for calculating the emergy input from Earth processes to landforms will have to be done differently based on results in this study. Because radioactive decay in the Earth's crust does not contribute to the available energy driving the Earth Cycle, future emergy evaluations should remove the heat generated by radioactivity from the heat flux measured in bore holes before applying the transformity for Earth heat to estimate the emergy inflow. Estimates of heat generation from radioactive decay are often reported with heat flux measurements. Also, an appropriate Carnot ratio should be applied to this heat flow to obtain available energy before multiplying by the transformity of deep Earth heat as proposed earlier by Brown and Ulgiati (2010).

5.12. A check on the primary calculation used to estimate the solar transformity of tidal exergy

In theory, the transformity of a process obtained from applying Euclid's Axiom can be checked by analyzing another process to which the two quantities also contribute. However, prior to this study, a second global process that could be used to check a value obtained from an evaluation of a first process was not known. As described above, the solar transformity of tidal exergy was checked by relating the kinetic energy of plate movements driven by deep Earth heat to the kinetic energy of the lithosphere rotated westward over the mantle by tidal forces. This method gave plausible results when compared to the estimate of the transformity of the tides derived from an analysis of the work of solar radiation and the gravitational attraction of the Moon and Sun in generating the geopotential energy of the world oceans. Although the second calculation that was used to check the first had a large uncertainty, the most probable value corresponded closely to the estimate of the solar transformity of the tides obtained from the first method. When similar values are obtained by this method of "triangulating" on the value of a transformity (Bastianoni et al., 2005) confidence in a calculation is increased and uncertainty is reduced, because of the mutual reinforcement of predictions generated by independent evaluations of different processes.

6. Conclusions

Emergy evaluation provides a universal accounting system that can be applied to determine the value of all quantities that have a known production function in terms of the available energy and emergy required to have that quantity as a part of the system. The available energy of all quantities within the geobiosphere of the Earth can be converted to emergy through multiplication by an appropriate transformity (sej J^{-1}), which has been established by evaluating a production process relative to the Earth's planetary solar equivalent energy baseline.

In this paper, the fundamental epistemological obstacle to establishing a unified planetary baseline was overcome by using the transitive property of equalities to estimate the equivalences between solar exergy and the Earth's deep heat exergy flow (4200 seJ J^{-1}) and between solar exergy and the exergy dissipated by the tides in the world oceans (35,400 seJ J^{-1}). The planetary baseline for the present condition of the Earth, i.e., with ice-covered polar oceans, was found to be 1.16×10^{25} seJ y^{-1} with the organizing power of the inputs distributed as follows: 1/3 solar radiation, 1/3 deep Earth heat and 1/3 tidal geopotential energy.

The time history of variations in the planetary baseline was calculated and it was found to have been remarkably stable over the past 555,000,000 y (i.e., $1.00 \times 10^{25} \pm 1.13 \times 10^{24}$ seJ y^{-1} or ± about 11%). The primary way that the Earth Cycle affects the geopotential energy dissipated in the world oceans is through the effect of the position of the continents on the harmonic resonance of the ocean basins. Over the past 5.55×10^{8} y the relative efficiency of the Earth as a "machine" for generating tidal geopotential exergy has varied from 31% to 155% of its present value.

Analysis of the data uncertainty associated with this baseline estimate, e.g., ±5% in the estimate of the deep heat flow supporting the Earth Cycle, indicates that this estimate of the baseline is within the ±15% or better bounds for data quality recommended for emergy evaluations (Campbell and Ohrt, 2009). However, model uncertainty can introduce larger errors, e.g., the standard deviation of the 5 baselines estimates made using different models was ±24%.

In this paper, a major error and a minor error in the data used in earlier calculations were corrected. Also, an argument based on geophysical considerations was presented that the highly aggregated models of the Earth system used by Odum (2000), Brown and Ulgiati (2010) and Campbell et al. (2010) do not give accurate equivalences between solar radiation and deep Earth heat or between solar radiation and tidal geopotential energy that are valid on the temporal scale of an annual emergy evaluation.

The close correspondence of the properties of the new baseline with the predictions made using the principles of EST indicate that the baseline is not really arbitrary and that this new baseline should be preferred over prior determinations. After the arguments presented in this paper are vetted by the community of concerned scientists and compared with other models for the estimation of the baseline, emergy researchers might settle on a value close to 1.16×10^{25} seJ y^{-1} as a plausible and agreed upon value of the planetary emergy baseline to be applied in subsequent emergy evaluations. Considering the variability of the historical baseline (±11.3%) and the uncertainty in the determinations of the Earth heat flux of ±5% the value of the baseline could be rounded to 1.2×10^{25} seJ y^{-1}, which also conforms with the average of the baseline estimates in three current studies of the emergy baseline of the planet (Brown and Ulgiati, DeVilbiss et al. and this study).

Acknowledgements

Although the research described in this article has been funded by the United States Environmental Protection Agency (USEPA), it has not been subjected to Agency level review; therefore, it does not necessarily reflect the views of the Agency. This article is Office of Research and Development contribution number ORD-011629. Dr. Hongfang Lu of South China Botanical Garden, Chinese Academy of Sciences, provided support for this work discussions and through electronically reading data from figures in Sorokhtin et al. (2011). Drs. Giancarlo Cicchetti, Peg Pelletier, and Hal Walker, Tim Gleason

and Wayne Munns all of NHEERL's Atlantic Ecology Division, provided helpful technical reviews of the paper. Joe Livolsi, also of AED performed the QA review. Giancarlo Cicchetti and Cissy Ma (USEPA, NRMRL) improved the paper through extensive comments. Giancarlo suggested the title, which was subsequently modified by Tim Gleason in review.

Appendix A. Tables of historical data used in calculating the emergy baseline of the Earth over the past 555,000,000 years

In Appendix A, large numbers are written in exponential format commonly used in engineering studies, instead of scientific notation. For example, one million = 1.0E + 6 = 1.0×10^6 (Tables A1–A5).

Table A1
Estimates of the available energy of the ocean tides based on the past history of the M_2 tidal component in terawatts over the last 1.0×10^9 years (Kagan, 1997) and earlier based on a model of tidal resonance (Kagan and Maslova, 1994).

Time period	Time years 10^6 BP	M_2 average[a] (TW)	Ocean tides[b] (TW)	Available energy ocean tides[c] (J y^{-1})
Archean[d]	2500	3.689	3.500	1.10E + 20
Paleo Proterozoic[d]	2000	1.660	1.575	4.97E + 19
Meso Proterozoic[d]	1500	1.402	1.330	4.20E + 19
Early Ryphean	1000	2.090	2.881	9.09E + 19
Late Ryphean	800	4.740	5.934	1.87E + 20
Wendian	600	2.360	3.192	1.01E + 20
Early Cambrian	555	4.300	5.427	1.71E + 20
Late and Middle Ordovician	465	3.875	4.937	1.56E + 20
Late Ordovician	450	3.500	4.505	1.42E + 20
Middle Silurian	420	2.900	3.814	1.20E + 20
Middle and Early Devonian	380	1.185	1.838	5.80E + 19
Early Carboniferous	335	1.100	1.740	5.49E + 19
Late Carboniferous	307.5	0.820	1.418	4.47E + 19
Early Permian	280	0.540	1.095	3.46E + 19
Triassic	202.5	1.203	1.858	5.86E + 19
Late and Middle Jurassic	147.5	0.830	1.429	4.51E + 19
Middle Cretaceous	97.5	1.775	2.518	7.95E + 19
Late Cretaceous	70	1.600	2.316	7.31E + 19
Early Paleocene	63	1.550	2.259	7.13E + 19
Early Eocene	53	1.390	2.074	6.55E + 19
Late and Middle Eocene	47	3.120	4.067	1.28E + 20
Early Oligocene	38	2.230	3.042	9.60E + 19
Early Miocene	20	1.360	2.040	6.44E + 19
Late Miocene	10	2.415	3.255	1.03E + 20
Present	0	2.628	3.500	1.10E + 20

[a] Average values of the major lunar semidiurnal tidal component, M_2, were obtained by averaging the estimates from four sources (i.e., Gotlib and Kagan, 1985, 1988; Kagan and Kivman, 1995; Ooe, 1989; Sundermann and Brosche, 1978) given in Kagan (1997).

[b] The available energy of ocean tides was estimated from the average values of the M_2 tidal component by first adjusting the M_2 estimate to account for the additional lunar components of the tide by multiplying it by the ratio (1.314) of all lunar components (3.2 TW) from Munk and Wunsch (1998) to current measurements of the M_2 tidal energy dissipation (2.436 TW) obtained from satellite altimetry data (Egbert and Ray, 2000). Then Kagan (1997)'s average M_2 value for the present was normalized to the satellite altimetry observations by multiplying it by 0.927. Next, the solar component of the tides (0.5 TW) from Munk and Wunsch (1998) was added assuming that it has been relatively constant over time. Finally, the Earth tide was subtracted, which was assumed to be the same fraction of the total tidal energy (0.054) over time as that found by Munk and Wunsch (1998), to obtain the available energy of the ocean tides from 2500×10^6 y BP to the present.

[c] The ocean tides in TW were multiplied by 10^{12} and the number of seconds in a year to convert TW to J y^{-1}.

[d] Tidal energies dissipated in the Archean and the Meso and Paleo Proterozoic Eras were estimated as multiples of the present value. The values of the multiples came from the reference line using a resonance lifetime of 0.02 in model of Kagan and Maslova (1994). The reference line was normalized by the consolidation-disintegration cycle of the continents (Fig. 3 in Kagan, 1997).

Table A2
Estimates of the transformity of the available energy of ocean tides based on the solar part of the total dissipation of geopotential energy in the world oceans. Solar transformities of the tide are estimated over the past 2.5×10^9 years based on both the solar energy received at the top of the atmosphere, R_r, and the solar energy absorbed at the Earth's surface, R_a. The solar transformity of the ocean tides is reported for an Earth with polar ice (3.8×10^7 years BP to the present) and without polar ice (2.5×10^9 years to 3.8×10^7 years BP). The transformity of the ocean tides is also reported based on the relative efficiency of the Earth as a "machine" for generating tidal exergy.

Time years 10^6 BP	R_r, solar received (J y^{-1})	R_a, solar absorbed (J y^{-1})	Total tide (J y^{-1})	Ocean tides (J y^{-1})	Total[a] dissipation (J y^{-1})	Solar part[b] (J y^{-1})	Solar Equiv. ocean tide, R_a (seJ J^{-1})	Solar Equiv. ocean tide R_r (seJ J^{-1})	Rel. efficiency[c] equivalence R_a (seJ J^{-1})
2500	5.1E + 24	3.57E + 24	1.16E + 20	1.10E + 20	2.59E + 20	1.48E + 20	24,111	34,445	28,020
2000	5.18E + 24	3.63E + 24	5.24E + 19	4.97E + 19	2.00E + 20	1.50E + 20	24,111	34,445	62,266
1500	5.26E + 24	3.68E + 24	4.42E + 19	4.20E + 19	1.95E + 20	1.53E + 20	24,111	34,445	73,737
1000	5.34E + 24	3.74E + 24	9.61E + 19	9.09E + 19	2.46E + 20	1.55E + 20	24,111	34,445	34,043
800	5.36E + 24	3.75E + 24	1.98E + 20	1.87E + 20	3.43E + 20	1.56E + 20	24,111	34,445	16,528
600	5.38E + 24	3.76E + 24	1.06E + 20	1.01E + 20	2.57E + 20	1.56E + 20	24,111	34,445	30,725
555	5.4E + 24	3.78E + 24	1.81E + 20	1.71E + 20	3.28E + 20	1.57E + 20	24,111	34,445	18,071
500	5.42E + 24	3.79E + 24	1.73E + 20	1.64E + 20	3.21E + 20	1.57E + 20	24,111	34,445	18,925
465	5.42E + 24	3.8E + 24	1.65E + 20	1.56E + 20	3.13E + 20	1.57E + 20	24,111	34,445	19,863
450	5.43E + 24	3.8E + 24	1.50E + 20	1.42E + 20	3.00E + 20	1.58E + 20	24,111	34,445	21,768
420	5.43E + 24	3.8E + 24	1.27E + 20	1.20E + 20	2.78E + 20	1.58E + 20	24,111	34,445	25,713
380	5.44E + 24	3.81E + 24	6.13E + 19	5.80E + 19	2.16E + 20	1.58E + 20	24,111	34,445	53,352

Table A2 (*Continued*)

Time years 10^6 BP	R_r, solar received ($J\,y^{-1}$)	R_a, solar absorbed ($J\,y^{-1}$)	Total tide ($J\,y^{-1}$)	Ocean tides ($J\,y^{-1}$)	Total[a] dissipation ($J\,y^{-1}$)	Solar part[b] ($J\,y^{-1}$)	Solar Equiv. ocean tide, R_a (seJ J^{-1})	Solar Equiv. ocean tide R_r (seJ J^{-1})	Rel. efficiency[c] equivalence R_a (seJ J^{-1})
335	5.44E+24	3.81E+24	5.81E+19	5.49E+19	2.13E+20	1.58E+20	24,111	34,445	56,354
307.5	5.45E+24	3.81E+24	4.73E+19	4.47E+19	2.03E+20	1.58E+20	24,111	34,445	69,177
280	5.45E+24	3.82E+24	3.65E+19	3.46E+19	1.93E+20	1.58E+20	24,111	34,445	89,554
202.5	5.47E+24	3.83E+24	6.20E+19	5.86E+19	2.17E+20	1.59E+20	24,111	34,445	52,773
147.5	5.47E+24	3.83E+24	4.77E+19	4.51E+19	2.04E+20	1.59E+20	24,111	34,445	68,620
97.5	5.48E+24	3.84E+24	8.40E+19	7.95E+19	2.39E+20	1.59E+20	24,111	34,445	38,949
70	5.49E+24	3.84E+24	7.73E+19	7.31E+19	2.32E+20	1.59E+20	24,111	34,445	42,340
63	5.49E+24	3.84E+24	7.54E+19	7.13E+19	2.31E+20	1.59E+20	24,111	34,445	43,419
53	5.49E+24	3.84E+24	6.92E+19	6.55E+19	2.25E+20	1.59E+20	24,111	34,445	47,278
47	5.49E+24	3.84E+24	1.36E+20	1.28E+20	2.88E+20	1.59E+20	24,111	34,445	24,111
38	5.49E+24	3.84E+24	1.01E+20	9.60E+19	2.05E+20	1.09E+20	35,358	50,511	40,681
20	5.5E+24	3.85E+24	6.80E+19	6.44E+19	1.73E+20	1.09E+20	35,358	50,511	60,670
10	5.5E+24	3.85E+24	1.09E+20	1.03E+20	2.12E+20	1.09E+20	35,358	50,511	38,017
0	5.5E+24	3.85E+24	1.17E+20	1.10E+20	2.19E+20	1.09E+20	35,358	50,511	35,358

[a] Total dissipation of geopotential energy in the world oceans is the sum of the available energy of the ocean tide and the available energy of the solar part. The available energy of the ocean tides was calculated in Table A1 from data in Kagan (1997).

[b] The solar part of the geopotential energy of the oceans was determined for an Earth with and without polar ice from data given in Tables 5 and 6. The efficacy of solar energy absorbed in creating the geopotential of the world oceans was allowed to vary over time under the assumption that as the solar radiation absorbed increased there would be a proportionate increase in the solar part of the available energy of the ocean geopotential.

[c] The transformities of the tides based on the solar exergy absorbed for the two modes (i.e., with and without polar ice) were modified by the relative efficiency of the configuration of the continents in generating tidal exergy in each mode to obtain the transformities listed in this column. For example, the ratio of the tidal exergy dissipated at time, t, to the tidal exergy dissipated at time, t_0, of a mode (0 or 38×10^6 y BP) was multiplied by the solar transformity of the tide at t_0 for that mode to give the transformities in column 10.

Table A3
Estimates of the available energy dissipated by land erosion over the last 542,000,000 years. The calculations in this table are based on the potential energy degraded to heat by a mass falling through a distance (Verhoogen, 1980) or $U = gmh$. In this table m converted to kilograms is the erosion mass flux, h in meters is the average height of the continents, and g is equal to 9.81 $m\,s^{-2}$. The product was multiplied by 0.5 to adjust for the center of the mass eroded to give the potential energy degraded to heat by erosion of the continents. Data are from Wilkinson and McElroy (2006) except as noted.

Time period	Time years 10^6 BP	Area of continents 10^6 km^2	Sediment deposited 10^6 km^3 my^{-1}	Erosion rate ($m\,my^{-1}$)	Erosion[a] mass flux ($t\,y^{-1}$)	Height[b] continent (m)	Exergy of erosion ($J\,y^{-1}$)
Lower Cambrian	542	81.196	0.750	9.24	2.10E+09	779	8.02E+15
Middle Cambrian	521	104.961	1.062	10.12	2.97E+09	780	1.14E+16
Upper Cambrian	499	71.789	1.955	27.23	5.47E+09	780	2.09E+16
Ordovician	488.3	76.868	0.883	11.49	2.47E+09	781	9.47E+15
Silurian	443.7	76.879	1.245	16.20	3.49E+09	782	1.34E+16
Lower Devonian	416	97.992	1.030	10.51	2.88E+09	783	1.11E+16
Middle Devonian	397.5	101.544	1.056	10.40	2.96E+09	783	1.14E+16
Upper Devonian	385.3	113.043	1.424	12.59	3.99E+09	783	1.53E+16
Lower Carboniferous	345.3	117.630	0.976	8.30	2.73E+09	784	1.05E+16
Upper Carboniferous	318.1	123.078	0.557	4.53	1.56E+09	812	6.21E+15
Lower Permian	299	131.126	0.662	5.05	1.85E+09	812	7.39E+15
Upper Permian	270.6	144.157	2.778	19.27	7.78E+09	813	3.10E+16
Lower Triassic	251	138.665	1.759	12.69	4.93E+09	814	1.97E+16
Middle Triassic	245.9	133.034	0.585	4.40	1.64E+09	814	6.54E+15
Upper Triassic	228.7	142.200	1.213	8.53	3.40E+09	815	1.36E+16
Lower Jurassic	199.6	133.739	0.791	5.92	2.22E+09	815	8.86E+15
Middle Jurassic	175.6	137.916	1.002	7.27	2.81E+09	828	1.14E+16
Upper Jurassic	161.2	139.609	1.841	13.19	5.16E+09	835	2.11E+16
Lower Cretaceous	140.2	113.860	2.634	23.14	7.38E+09	843	3.05E + 16
Upper Cretaceous	99.6	134.087	3.390	25.28	9.49E+09	844	3.93E+16
Tertiary-Paleocene	65	130.228	4.776	36.68	1.34E+10	845	5.54E+16
Tertiary-Eocene	55.8	139.165	3.176	22.83	8.89E+09	851	3.71E+16
Tertiary-Oligocene	33.9	142.231	3.128	21.99	8.76E+09	864	3.71E+16
Tertiary-Miocene	23.03	139.519	2.417	17.33	6.77E+09	871	2.89E+16
Tertiary Pliocene	5.332	144.117	7.669	53.21	2.15E+10	852	8.98E+16
Pleistocene[c]	2.588	139.413	8.644	62.00	2.07E+10	873	8.86E+16
Holocene[d]	0.0117	134.709	58.464	434.00	6.30E+10	840	2.60E+17

[a] Density of the continental crust was assumed to be 2.8 g/cc (Condie, 1993)

[b] Data from Sorokhtin et al. (2011).

[c] Data on the Pleistocene erosion mass flux is taken form a separate data base on sediment carried by large rivers in Wilkinson and McElroy (2006).

[d] Numbers in this row include estimates of erosion from agricultural lands.

Table A4
Determination of the solar equivalence of Earth Cycle exergy by equating the solar exergy of erosion with the Earth heat equivalence of total uplift (isostatic adjustment plus uplift from plate movement). Data on Earth heat flows and temperatures from Sorokhtin et al. (2011). The erosion exergy in red and underlined is based on river sediment flux.

Time Years 10^9BP	Solar Ex. Absorbed J y^{-1}	Earth Cycle Heat Flow[a] J y^{-1}	Mantle Temp[b] °K	Sea floor Temp[c] °K	Carnot Ratio[d]	Earth Cycle Exergy[e] J y^{-1}	Exergy of Erosion[f] J y^{-1}	S. Equiv. Erosion[g] seJ J^{-1}	E. H.Trans. Uplift[h] eeJ J^{-1}	Solar Equiv. Earth Exergy[i] seJ J^{-1}
0.555	3.785E+24	1.417E+21	2368.2	303.0	0.8720	1.235E+21	8.02E+15	4.72E+08	1.54E+05	3064
0.542	3.788E+24	1.409E+21	2367.5	302.6	0.8722	1.229E+21	8.02E+15	4.72E+08	1.53E+05	3083
0.521	3.790E+24	1.396E+21	2366.8	302.1	0.8724	1.218E+21	1.14E+16	3.33E+08	1.07E+05	3112
0.500	3.792E+24	1.383E+21	2366.1	301.6	0.8725	1.207E+21	2.09E+16	1.81E+08	5.76E+04	3143
0.488	3.792E+24	1.375E+21	2365.5	301.1	0.8727	1.200E+21	9.47E+15	4.01E+08	1.27E+05	3159
0.465	3.792E+24	1.360E+21	2364.8	300.6	0.8729	1.188E+21	1.08E+16	3.50E+08	1.10E+05	3193
0.450	3.792E+24	1.351E+21	2364.1	300.1	0.8731	1.179E+21	1.22E+16	3.10E+08	9.64E+04	3216
0.444	3.792E+24	1.345E+21	2363.4	299.6	0.8733	1.174E+21	1.34E+16	2.84E+08	8.78E+04	3229
0.420	3.792E+24	1.322E+21	2362.7	299.1	0.8734	1.155E+21	1.19E+16	3.18E+08	9.67E+04	3283
0.416	3.792E+24	1.318E+21	2362.1	299.0	0.8734	1.152E+21	1.11E+16	3.43E+08	1.04E+05	3293
0.398	3.792E+24	1.302E+21	2361.4	297.8	0.8739	1.138E+21	1.14E+16	3.34E+08	1.00E+05	3333
0.385	3.792E+24	1.291E+21	2360.7	296.7	0.8743	1.129E+21	1.53E+16	2.48E+08	7.37E+04	3360
0.380	3.792E+24	1.286E+21	2360.0	295.5	0.8748	1.125E+21	1.29E+16	2.94E+08	8.71E+04	3370
0.345	3.792E+24	1.261E+21	2359.3	294.3	0.8753	1.104E+21	1.05E+16	3.61E+08	1.05E+05	3436
0.335	3.792E+24	1.253E+21	2358.7	293.2	0.8757	1.098E+21	8.36E+15	4.53E+08	1.31E+05	3454
0.318	3.792E+24	1.243E+21	2358.0	293.8	0.8754	1.088E+21	6.21E+15	6.11E+08	1.75E+05	3484
0.308	3.792E+24	1.237E+21	2357.3	294.5	0.8751	1.083E+21	6.80E+15	5.58E+08	1.59E+05	3503
0.299	3.792E+24	1.232E+21	2356.6	295.1	0.8748	1.078E+21	7.39E+15	5.13E+08	1.46E+05	3518
0.280	3.792E+24	1.221E+21	2355.9	295.8	0.8744	1.067E+21	1.92E+16	1.97E+08	5.56E+04	3552
0.271	3.792E+24	1.212E+21	2355.3	296.5	0.8741	1.059E+21	3.10E+16	1.22E+08	3.41E+04	3579
0.251	3.792E+24	1.193E+21	2354.6	297.1	0.8738	1.043E+21	1.97E+16	1.93E+08	5.30E+04	3636
0.246	3.792E+24	1.188E+21	2353.9	297.8	0.8735	1.038E+21	6.54E+15	5.80E+08	1.59E+05	3652
0.229	3.792E+24	1.163E+21	2353.2	298.4	0.8732	1.016E+21	1.36E+16	2.79E+08	7.49E+04	3732
0.203	3.792E+24	1.125E+21	2352.6	299.1	0.8729	9.823E+20	1.12E+16	3.38E+08	8.76E+04	3860
0.200	3.792E+24	1.124E+21	2351.9	299.8	0.8725	9.805E+20	8.86E+15	4.28E+08	1.11E+05	3867
0.176	3.791E+24	1.111E+21	2351.2	297.0	0.8737	9.705E+20	1.14E+16	3.33E+08	8.52E+04	3907
0.161	3.791E+24	1.103E+21	2350.5	294.3	0.8748	9.649E+20	2.11E+16	1.79E+08	4.57E+04	3929
0.148	3.791E+24	1.096E+21	2349.8	291.5	0.8759	9.597E+20	2.58E+16	1.47E+08	3.72E+04	3951
0.140	3.791E+24	1.092E+21	2349.2	288.8	0.8771	9.575E+20	3.05E+16	1.24E+08	3.14E+04	3960
0.100	3.791E+24	1.072E+21	2348.5	286.0	0.8782	9.418E+20	3.93E+16	9.65E+07	2.40E+04	4025
0.098	3.791E+24	1.071E+21	2347.8	285.3	0.8785	9.412E+20	4.47E+16	8.49E+07	2.11E+04	4028
0.070	3.791E+24	1.058E+21	2347.1	284.6	0.8787	9.301E+20	5.01E+16	7.57E+07	1.86E+04	4076
0.065	3.791E+24	1.056E+21	2346.4	284.0	0.8790	9.283E+20	5.54E+16	6.84E+07	1.67E+04	4084
0.063	3.791E+24	1.055E+21	2345.8	283.3	0.8792	9.277E+20	4.63E+16	8.19E+07	2.00E+04	4087
0.056	3.791E+24	1.052E+21	2345.1	282.6	0.8795	9.250E+20	3.71E+16	1.02E+08	2.49E+04	4099
0.053	3.791E+24	1.050E+21	2344.4	281.9	0.8797	9.241E+20	3.71E+16	1.02E+08	2.49E+04	4103
0.047	3.791E+24	1.048E+21	2343.7	281.3	0.8800	9.218E+20	3.71E+16	1.02E+08	2.48E+04	4113
0.038	3.791E+24	1.043E+21	2343.1	280.6	0.8803	9.183E+20	3.71E+16	1.02E+08	2.47E+04	4128
0.034	3.791E+24	1.041E+21	2342.4	279.9	0.8805	9.169E+20	3.71E+16	1.02E+08	2.47E+04	4135
0.023	3.791E+24	1.036E+21	2341.7	279.2	0.8808	9.126E+20	2.89E+16	1.31E+08	3.16E+04	4154
0.020	3.791E+24	1.035E+21	2341.0	278.5	0.8810	9.116E+20	4.92E+16	7.71E+07	1.85E+04	4159
0.010	3.791E+24	1.030E+21	2340.3	277.9	0.8813	9.077E+20	6.95E+16	5.46E+07	1.31E+04	4177
0.005	3.810E+24	1.028E+21	2339.7	277.2	0.8815	9.060E+20	8.98E+16	4.24E+07	1.01E+04	4206
0.003	3.830E+24	1.026E+21	2339.0	276.5	0.8818	9.051E+20	8.86E+16	4.32E+07	1.02E+04	4231
0.000	3.849E+24	1.025E+21	2338.3	276.5	0.8817	9.040E+20	2.60E+17	1.48E+07	3.48E+03	4258

(a) Earth Cycle heat flow is the energy of the Earth's deep heat flow driving tectonic movements of the Earth's plates and isostatic processes. These flows are based on the cold body theory of the Earth's formation and can be found in Figs. 5–17 of Sorokhtin et al. (2011). (b) Data on the average mantle temperature are from Fig. 5.15 in Sorokhtin et al. (2011). (c) Data on sea floor temperature is from Fig. 14.1 in Sorokhtin et al. (2011). (d) The Carnot ratio is the difference between the average mantle and the ocean bottom temperatures divided by the average mantle temperature. It indicates the fraction of the Earth's deep heat flow that is available to do work in the system. (e) The Earth Cycle heat flow times the Carnot ratio gives the available energy driving the Earth's tectonic processes. (f) The available energy of erosion is calculated in Table A3. The exergy of erosion at 555×10^6 y BP was assumed equal to that at 542×10^6 y BP. (g) The solar exergy equivalence of erosion is the solar available energy flow absorbed at the Earth's surface divided by the available energy of the mass removed by erosion (seJ J^{-1}). (h) The Earth heat equivalence of the mass uplifted is equal to the Earth Cycle's available energy flow divided by the available energy of the mass eroded, under the assumption that the available energy of the mass eroded is equal to the available energy of the mass uplifted to replace it over geologic time (e.g., 10 million years). (i) The solar exergy equivalence of the Earth Cycle available energy flow is estimated by forming the ratio of the solar exergy of the available energy of the mass eroded to the Earth heat equivalence of the available energy of the mass uplifted under the assumption that the same mass, and therefore, the same available energy equivalent is being both eroded and uplifted over geologic time.

Table A5
Planetary emergy baseline for the Earth from 555,000,000 y BP to the present.

Time years 10^9 BP	Solar exergy ($J\,y^{-1}$)	Earth cycle exergy ($J\,y^{-1}$)	Ocean tidal exergy ($J\,y^{-1}$)	Solar equivalence Earth cycle ($seJ\,J^{-1}$)	Solar equivalence tidal exergy ($seJ\,J^{-1}$)	Planetary baseline ($seJ\,y^{-1}$)
0.555	3.778E+24	1.235E+21	1.713E+20	3064	24,111	1.169E+25
0.500	3.792E+24	1.207E+21	1.635E+20	3083	24,111	1.146E+25
0.465	3.796E+24	1.188E+21	1.558E+20	3193	24,111	1.135E+25
0.450	3.798E+24	1.179E+21	1.422E+20	3216	24,111	1.102E+25
0.420	3.801E+24	1.155E+21	1.204E+20	3283	24,111	1.050E+25
0.380	3.806E+24	1.125E+21	5.801E+19	3370	24,111	8.997E+24
0.335	3.811E+24	1.098E+21	5.492E+19	3454	24,111	8.927E+24
0.308	3.814E+24	1.083E+21	4.474E+19	3503	24,111	8.685E+24
0.280	3.817E+24	1.067E+21	3.456E+19	3552	24,111	8.442E+24
0.203	3.826E+24	9.823E+20	5.864E+19	3860	24,111	9.032E+24
0.148	3.832E+24	9.597E+20	4.510E+19	3951	24,111	8.711E+24
0.098	3.838E+24	9.412E+20	7.946E+19	4028	24,111	9.545E+24
0.070	3.841E+24	9.301E+20	7.310E+19	4076	24,111	9.395E+24
0.063	3.842E+24	9.277E+20	7.128E+19	4087	24,111	9.352E+24
0.053	3.843E+24	9.241E+20	6.546E+19	4103	24,111	9.213E+24
0.047	3.844E+24	9.218E+20	1.284E+20	4113	24,111	1.073E+25
0.038	3.845E+24	9.183E+20	9.600E+19	4128	35,358	1.103E+25
0.020	3.847E+24	9.116E+20	6.437E+19	4159	35,358	9.914E+24
0.010	3.848E+24	9.077E+20	1.027E+20	4177	35,358	1.127E+25
0.000	3.849E+24	9.040E+20	1.105E+20	4258	35,358	1.160E+25
Average	3.82E+24	1.03E+21	9.20E+19	3733	26,361	1.00E+25

Appendix B. Comparison of the solar equivalent exergy ratios obtained in this study to simple ratios of the same energy flows

Table B1.

Table B1
Comparison of solar, Earth and tidal energy flows and the solar energy to earth and tidal energy ratios with the exergy flows and estimates of the solar exergy equivalences of Earth's deep heat exergy driving tectonic processes, and the tidal exergy dissipated in the present (ice-covered oceans) and past (ice-free oceans) that were made in this study.

Solar energy[a]	Earth cycle energy[b]	Tidal energy[c]	Solar exergy[d]	Earth cycle exergy[e]	Tidal exergy, ice[f]	Tidal exergy ice-free[g]
3.86E+24	1.37E+21	1.17E+20	3.85E+24	9.20E+20	1.09E+20	1.60E+20
Dimensionless energy ratios			Equivalences ($seJ\,J^{-1}$)			
	Solar to Earth energy	Solar to tidal energy		Earth deep heat exergy	Tidal exergy, ice	Tidal exergy, ice-free
	2809	32,957		4190	35,394	24,166
Percent difference from simple energy ratios						
			0.04%	49.15%	7.39%	26.68%

[a] Table 4.
[b] Table 7.
[c] Table 2.
[d] Table 5.
[e] Table 2.
[f] Table 6.
[g] Table 6.

References

Anderson, D.L., 2005. Energetics of the Earth and The Missing Heat Source Mystery, From ⟨http://www.mantleplumes.org/Energetics.html⟩ (last accessed on Dec. 2, 2014).

Bastianoni, S., Campbell, D.E., Susani, L., Tiezzi, E., 2005. Ecol. Modell. 186, 212–220.

Bostrom, R.C., 1971. Westward displacement of the lithosphere. Nature 234, 536–538.

Breidert, C., Hahsler, M., Reutterer, T., 2006. A review of methods for measuring willingness-to-pay. Innovative Mark. 2 (4), 8–32, From ⟨http://businessperspectives.org/journals_free/im/2006/im_en_2006_04_Breidert.pdf⟩ (last accessed on April 1, 2015).

Brown, M.T., Ulgiati, S., 2010. Updated evaluation of exergy and emergy driving the geobiosphere: a review and refinement of the emergy baseline. Ecol. Modell. 221, 2501–2508.

Brown, M.T., Ulgiati, S., 2016. Assessing the global environmental sources driving the geobiosphere: a revised emergy baseline. Ecol. Modell. 339, 126–132.

Campbell, D.E., 1984. Energy Filter Properties of Ecosystems. University of Florida, Gainesville, FL, pp. 20, PhD. Dissertation.

Campbell, D.E., 1998. Emergy analysis of human carrying capacity and sustainability: an example using the State of Maine. Environ. Monit. Assess. 51, 531–569.

Campbell, D.E., 2000a. A revised solar transformity for tidal energy received by the earth and dissipated globally: implications for emergy analysis. In: Brown, M.T. (Ed.), Emergy Synthesis: Theory and Applications of Emergy Analysis. Proceedings of the First Biennial Emergy Analysis Research Conference. University of Florida, Gainesville, FL, pp. 255–264.

Campbell, D.E., 2000b. Using energy systems theory to define, measure, and interpret ecological integrity and ecosystem health. Ecosyst. Health 6 (3), 181–204.

Campbell, D.E., 2001. Proposal for including what is valuable to ecosystems in environmental assessments. Environ. Sci. Technol. 35 (14), 2867–2873.

Campbell, D.E., 2003. A note on the uncertainty in estimates of transformities based on global water budgets. In: Brown, M.T., Odum, H.T., Tilley, D., Ulgiati, S. (Eds.), Emergy Synthesis 2. Proceedings of the Second Biennial Emergy Analysis Conference. Center for Environmental Policy. University of Florida, Gainesville, FL, pp. 349–353.

Campbell, D.E., 2014. Environmental goods and services: economic and non-economic methods for valuing. In: Wang, Y.Q. (Ed.), Encyclopedia of Natural Resources: Land. Taylor and Francis, New York, NY, pp. 195–200, Published online: 21 Oct 2014.

Campbell, D.E., Odum, H.T., 1998. Appendix B: Calculation of a revised solar transformity for tidal energy received and tidal energy dissipated globally. In: Campbell, D.E. (Ed.), Emergy Analysis of Human Carrying Capacity and Sustainability: An

Example Using the State of Maine, vol. 51. Environ. Monit. Assess., pp. 531–569, p566.
Campbell, D.E., Ohrt, A., 2009. Environmental accounting using emergy: evaluation of Minnesota. In: USEPA Project Report. EPA 600/R-09/002., pp. 138.
Campbell, D.E., Brandt-Williams, S.L., Cai, T.T., 2005. Current technical problems in emergy analysis. In: Brown, M.T., Bardi, E., Campbell, D.E., Comar, V., Huang, S-L., Rydberg, T., Tilley, D.R., Ulgiati, S. (Eds.), Emergy Synthesis 3, Proceedings of the Third Biennial Emergy Research Conference, The Center for Environmental Policy. University of Florida, Gainesville, FL, pp. 143–157.
Campbell, D.E., Bastianoni, S., Lu, H.F., January 14–16, 2010. The emergy baseline of the Earth: is it arbitrary? A poster presentation at Emergy Synthesis 6. In: Proceedings of the Sixth Biennial Emergy Research Conference, The Center for Environmental Policy. University of Florida, Gainesville, FL.
Campbell, D.E., Lu, H.F., Lin, B.L., 2014. Emergy evaluations of the global biogeochemical cycles of six biologically active elements and two compounds. Ecol. Modell. 271, 32–51.
Carlson, R.L., Raskin, G.S., 1984. Density of the ocean crust. Nature 311, 555–558.
Chen, G.Q., 2005. Exergy consumption of the Earth. Ecol. Modell. 184, 363–380.
Chen, H., Chen, G.Q., Ji, X., 2010. Cosmic exergy based ecological systems modelling. Commun. Nonlinear Sci. Numer. Simul. 15, 2672–2700.
Christensen, N.I., Mooney, W.D., 1995. Seismic velocity structure and composition of the continental crust: a global view. J. Geophys. Res. 100 (B7), 9761–9788.
Collins, D., Odum, H.T., 2000. Calculating transformities with an eigenvector method. In: Brown, M.T., Brandt-Williams, S., Tilley, D., Ulgiati, S. (Eds.), Emergy Synthesis, Theory and Applications of the Emergy Methodology, Proceedings of the First Biennial Emergy Analysis Research Conference, Center for Environmental Policy. University of Florida, Gainesville, FL, pp. 265–280.
Comiso, J.C., 2002. A rapidly declining perennial sea ice cover in the Arctic. Geophys. Res. Lett. 29 (20), 17-1–17-4, 1956.
Condie, K.C., 1993. Chemical composition and evolution of the upper continental crust: contrasting results from surface samples and shales. Chem. Geol. 104, 1–37.
Conrad, C.P., Lithgow-Bertelloni, C., 2007. Faster seafloor spreading and lithosphere production during the mid-Cenozoic. Geology 35 (1), 29–32.
Corliss, J.B., Dymond, J., Gordon, L.I., Edmond, J.M., von Herzen, R.P., Ballard, R.D., Green, K., et al., 1979. Submarine thermal springs on the Galapagos Rift. Science 203, 1073–1083.
Davies, J.H., Davies, D.R., 2010. Earth's heat flux. Solid Earth 1, 5–24.
Deconto, R.M., Pollard, D., 2003. Rapid cenozoic glaciation of Antarctica induced by declining atmospheric CO_2. Nature 471, 245–249.
Doglioni, C., Carminati, E., Crespi, M., Cuffaro, M., Penati, M., Riguzzi, F., 2014. Tectonically asymmetric Earth: from net rotation to polarized westward drift of the lithosphere. Geosci. Front., http://dx.doi.org/10.1016/j.gsf.2014.02.001.
Egbert, G.D., Ray, R.D., 2000. Significant dissipation of tidal energy in the deep ocean inferred from satellite altimeter data. Nature 405, 775–778.
Elderfield, H., Schultz, A., 1996. Mid-ocean ridge hydrothermal fluxes and the chemical composition of the ocean. Annu. Rev. Earth Planet. Sci. 24, 191–224.
Foukal, P., Fröhlich, Spruit, H., Wigley, T.M.L, 2006. Variations in solar luminosity and their effect on the Earth's climate. Nature 443, 162–166.
Fox, P.J., Ruddiman, W.F., Ryan, W.B.F., Heezen, B.C., 1970. The geology of the Caribbean crust. I: Beata Ridge. Tectonophysics 10, 495–513.
Gotlib, V.Yu., Kagan, B.A., 1985. A reconstruction of the tides in the paleoocean: results of a numerical experiment. Dtsch. Hydrogr. Z. B38 (2), 43–57.
Gotlib, V.Yu., Kagan, B.A., 1988. The evolution of the global ocean tides in the Cenozoic. Okeanologiya (Moscow) 28 (1), 17–24.
Heath, T.L., 1908. The Thirteen Books of Euclid's Elements, Vol. III, Books X-XIII. Cambridge University Press, Cambridge, From ⟨https://archive.org/details/thirteenbookseu03heibgoog⟩ (last accessed on December 5, 2014).
Hermann, W.A., 2006. Quantifying global exergy resources. Energy 31, 1685–1702.
Hofmeister, A.M., Criss, R.E., 2005. Earth's heat flux revised and linked to chemistry. Tectonophysics 395, 159–177.
ITACA, 2011. Part 2: Solar Energy Reaching the Earth's Surface, From ⟨http://www.itacanet.org/?s=Solar+energy+reaching+the+Earth%27s+surface⟩ (last accessed August 27, 2014).
Jaupart, C., Labrosse, S., Mareschal, J.-C., 2007. Temperatures, heat and energy in the mantle of the Earth. In: Bercovici, D., Schubert, G. (Eds.), Treatise on Geophysics, Mantle Dynamics, vol. 7. Elsevier, Amsterdam, pp. 253–303, From ⟨https://www.academia.edu/214137/Temperatures_Heat_and_Energy_in_the_Mantle_of_the_Earth⟩ (last accessed on February 11, 2015).
Kagan, B.A., 1997. Earth–Moon tidal evolution: model results and observational evidence. Prog. Oceanog. 40, 109–124.
Kagan, B.A., Kivman, G.A., 1995. Variations of the Earth's rotation as derived from numerical modelling tides in the paleoocean. Acta Geodesy Geophys. Hungary 80 (2–4), 135–145.
Kagan, B.A., Maslova, N.B., 1994. A stochastic model of the Earth–Moon tidal evolution accounting for cyclic variations of resonant properties of the ocean: an asymptotic solution. Earth, Moon Planets 66, 173–188.
Knopoff, L., 1972. Observation and inversion of surface-wave dispersion. In: Ritsema, A.R. (Ed.), The Upper Mantle. Techonophysics 13 (1–4), 497–519.
Knopoff, L., Leeds, A., 1972. Lithospheric momenta and the deceleration of the Earth. Nature 237, 93–95.
Labrosse, S., Jaupert, C., 2007. Thermal evolution of the Earth: secular changes and fluctuations of plate characteristics. Earth Planet. Sci. Lett. 260, 465–481.
Le Corre, O., Truffet, L., 2012. Exact computation of emergy based on a mathematical reinterpretation of the rules of emergy algebra. Ecol. Modell., 101–113.
Lotka, A.J., 1922a. Contribution to the energetics of evolution. Proc. Natl. Acad. Sci. 8, 147–151.
Lotka, A.J., 1922b. Natural selection as a physical principle. Proc. Natl. Acad. Sci. 8, 151–154.
Li, L.J., Lu, H.F., Campbell, D.E., Ren, H., 2010. Emergy algebra: improving matrix methods for calculating transformities. Ecol. Modell. 221, 411–422.
Lu, H.F., Campbell, D.E., Chen, J., Qin, P., Ren, H., 2007. Conservation and economic viability of nature reserves: an emergy evaluation of the Yancheng Biosphere Reserve. Biol. Conserv. 139, 415–438.
Mareschal, J.-C., Jaupart, C., Phaneuf, C., Perry, C., 2012. Geoneutrinos and the energy budget of the Earth. J. Geodyn. 54, 43–54.
Miller, G.R., 1966. The flux of tidal energy out of the deep oceans. J. Geophys. Res. 71 (10), 2485–2489.
Mooney, W.D., Laske, G., Masters, G., 1998. J. Geophys. Res. 103 (B1), 727–747.
Mottl, M.J., Wheat, C.G., 1994. Hydrothermal circulation through mid-ocean ridge flanks: fluxes of heat and magnesium. Geochim. Cosmochim. Acta 58 (10), 2225–2237.
Munk, W.H., Macdonald, G.J.F., 1960. The Rotation of the Earth. Cambridge University Press, Cambridge.
Munk, W., Wunsch, C., 1998. Abyssal recipes II: Energetics of tidal and wind mixing. Deep-Sea Res. I: Oceanogr. Res. Pap. 45, 1977–2010.
NASA, National Aeronautics and Space Administration. Solar System Exploration, 2014a. Planets, Sun, From ⟨http://solarsystem.nasa.gov/planets/profile.cfm?Object = Sun⟩ (last accessed on August 27, 2014).
NASA, National Aeronautics and Space Administration. Solar System Exploration Goddard Institute for Space Studies, 2014b. Table Data: Global and Hemispheric Monthly Means and Zonal Annual Means., From ⟨http://data.giss.nasa.gov/gistemp/⟩ (last accessed on August 27, 2014).
NASA, National Aeronautics and Space Administration. Solar System Exploration, 2014c. Universe 101, Tests of the Big Bang: The CMB, From ⟨http://wmap.gsfc.nasa.gov/universe/bb_tests_cmb.html⟩ (last accessed on August 27, 2014).
Odum, H.T., 1971. Environment, Power, and Society. Wiley, New York, NY, pp. 331pp.
Odum, H.T., 1978. Energy analysis, energy quality, and environment. In: Gilliland, M.W. (Ed.), Energy Analysis: A New Public Policy Tool. AAAS Selected Symposium, vol. 9. Westview Press Inc, Boulder, CO, pp. 55–87.
Odum, H.T., 1994. Ecological and General Systems: An Introduction to Systems Ecology. Univ. Colorado Press, Niwot, CO, pp. 644, Revised edition of Systems Ecology, An Introduction. 1983. John Wiley&Sons, New York. 644 p.
Odum, H.T., 1996. Environmental Accounting: Emergy and Environmental Decision Making. John Wiley and Sons, New York, NY, pp. 370p.
Odum, H.T., 2000. Handbook of Emergy Evaluation. Folio #2. Emergy of Global Processes. Center for Environmental Policy, Environmental Engineering Sciences. University of Florida, Gainesville, FL, pp. 30p.
Odum, H.T., Odum, E.C. (Eds.), 1983. Energy Analysis Overview of Nations. Working Paper. International Institute of Applied Systems Analysis, Laxenburg, Austria, p. 469 (WP-83-82).
Odum, H.T., Brown, M.T., Brandt-Williams, S.L., 2000. Handbook of Emergy Evaluation. Folio #1. Introduction and Global Budget. Center for Environmental Policy, Environmental Engineering Sciences. University of Florida, Gainesville, FL, pp. 16p.
Ojibwa, 2012. Native American Netroots, Indian Chiefs, From ⟨http://nativeamericannetroots.net/diary/1354⟩ (last assessed on January 7, 2015).
Ooe, M., 1989. Effects of configuration and bathymetry of the ocean on the tidal dissipation of the Earth's rotation. J. Phys. Earth 37, 345–355.
Oort, A.H., Ascher, S.C., Levitus, S., Peixoto, J.P., 1989. New estimates of the available potential energy in the world ocean. J. Geophys. Res. 94 (No. C3), 3187–3200.
Oort, A.H., Anderson, L.A., Peixoto, J.P., 1994. Estimates of the energy cycle of the oceans. J. Geophys. Res. 99 (No. C4), 7665–7688.
Parsons, B., Sclater, J.G., 1977. An analysis of the variation of ocean floor bathymetry and heat flow with age. J. Geophys. Res. 82 (5), 803–827.
Petela, R., 1964. Exergy of heat radiation. J. Heat Transfer 86 (2), 187–192.
Pollack, H.N., Hurter, S.J., Johnson, J.R., 1993. Rev. Geophys. 31 (3), 267–280.
Raugei, M.A., 2013. A different take on the emergy baseline —or can there really be any such thing. In: Brown, M.T., Sweeney, S. (Eds.), Emergy Synthesis 7, Theory and Applications of the Emergy Methodology. The Center for Environmental Policy. University of Florida, Gainesville, FL, pp. 61–66.
Ray, R.D., Eanes, R.J., Chao, B.F., 1996. Detection of tidal dissipation in the solid Earth by satellite tracking and altimetry. Nature 381, 595–597.
Riguzzi, F., Panza, G., Varga, P., Doglioni, C., 2009. Can Earth's rotation and tidal despinning drive plate tectonics? Tectonophysics 484, 60–73.
Rothrock, D.A., Zhang, J., 2005. Arctic ocean sea ice volume: what explains its recent depletion? J. Geophys. Res. 110, C01002-1–C-1012.
Runcorn, S.K., 1962. Convection currents in the Earth's mantle. Nature 195, 1248–1249.
Runcorn, S.K., 1965. Changes in the convection patterns in the Earth's mantle and continental drift: evidence for a cold origin of the Earth. Philos. Trans. R. Soc. Lond., Ser. A 258, 228–251.
Sackmann, I.J., Boothroyd, A.I., Kraemer, K.E., 1993. Our Sun. III. Present and future. Astrophys. J. 418, 457–468.
Safronov, V.S., 1969. Evolution of the Pre-planetary Cloud and the Formation of the Earth and planets. Nauka, Moscow, pp. 244 p.
Schmidt, O.Yu., 1946. New theory of Earth's origins. Nature 7, 6–16.
Schmidt, O.Yu., 1958. A Theory of Earth's Origin, Four Lectures. Foreign Languages Publishing House, Moscow, pp. 139p.
Scienceman, D.M., 1987. Energy and EMERGY. In: Pillet, G., Murota, T. (Eds.), Environmental Economics. Roland Leimgruber, Geneva, pp. 257–276.

Sclater, J.G., Jaupart, C., Galson, D., 1980. The heat flow through oceanic and continental crust and the heat loss of the Earth. Rev. Geophys. Space Phys. 18, 269–311.
Sorokhtin, O.G., 1974. Global Evolution of the Earth. Nauka, Moscow, pp. 184 p.
Sorokhtin, O.G., Dmitriyev, L.V., Udintsev, G.B., 1971. Possible mechanism of the Earth's crust formation. Proc. AN USSR 199, 2319–2322.
Sorokhtin, O.G., Chilingarian, G.V., Sorokhtin, N.O., 2011. Evolution of Earth and its Climate Birth, Life and Death of Earth. Developments in Earth & Environmental Sciences. Elsevier, Amsterdam, pp. 576.
Stein, C.A., Stein, S., 1994. Constraints on hydrothermal heat flux through the oceanic lithosphere from global heat flow. J. Geophys. Res. 99 (B2), 3018–3095.
Sundermann, J., Brosche, P., 1978. The numerical computation of tidal friction for present and ancient oceans. In: Broesche, P., Sundermann, J. (Eds.), Tidal Friction and the Earth's Rotation. Springer, Berlin, pp. 125–144.
Tennenbaum, S., 1988. Network Energy Expenditures for subsystem Production. Environmental Engineering Sciences, Univ. of Florida, Gainesville, pp. 132, M.S. Thesis.
Tilley, D.R., 2015. Transformity dynamics related to maximum power for improved emergy yield estimations. Ecol. Modell. 315, 96–107.
Verhoogen, J., 1980. Energetics of the Earth. National Academy of Sciences, Washington, DC, pp. 137, From ⟨http://www.nap.edu/openbook.php?record_id=9579&page=R1⟩ (last accessed on October 16, 2014).
Weast, R.C., 1981. CRC, Handbook of Chemistry and Physics. CRC Press, Inc, Boca Raton, FL.
Wetherill, G.W., 1990. Formation of the Earth. Ann. Rev. Earth Plant. Sci. 18, 205–256.
Wijesekera, H., Boyd, T.J., 2001. Upper Ocean Heat and Freshwater Budgets. Academic Press, Cambridge, MA, USA, pp. 3079–3083, From ⟨http://curry.eas.gatech.edu/Courses/6140/ency/Chapter9/Ency_Oceans/Upper_Ocean_Heat_Freshwater_Budgets.pdf⟩ (last accessed on December 4, 2014).
Wilkinson, B.H., McElroy, B.J., 2006. The impact of humans on continental erosion and sedimentation. Geol. Soc. Am. Bull. 119 (1/2), 140–156.
Williams, D.L., von Herzen, R.P., Sclater, J.G., Anderson, R.N., 1974. The Galapagos spreading centre: lithospheric cooling and hydrothermal circulation. Geophys. J. R. Astron. Soc. 38, 587–608.
Zachos, J., Pagani, M., Sloan, L., Thomas, E., Billups, K., 2001. Trends, rhythms, and aberrations in global climate 65 ma to present. Science 292, 686–690.